67p

GEMP-190n
(INFORMAL)
Part B

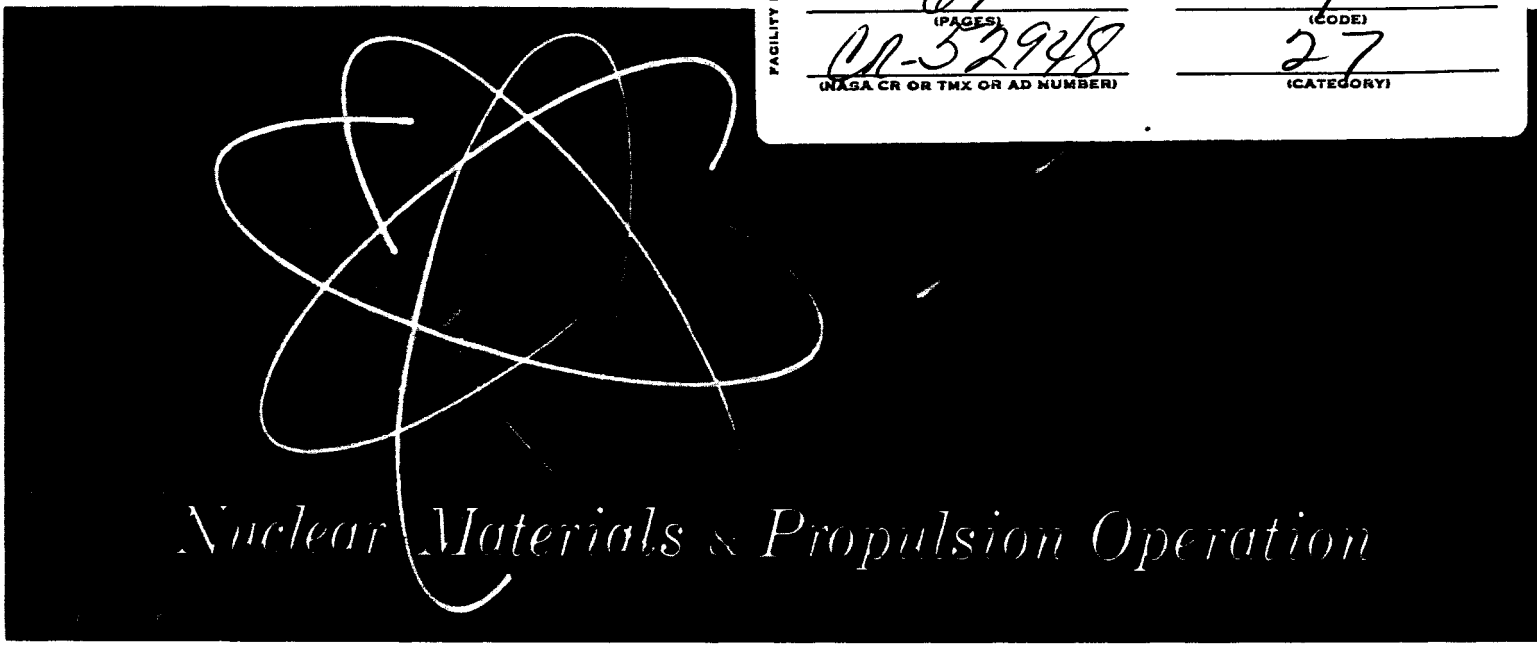

INTRODUCTION TO NUCLEAR PROPULSION

Lecture 21 - NUCLEAR ROCKET SYSTEM

Russell E. Motsinger

ADVANCED TECHNOLOGY SERVICES

GENERAL ELECTRIC

GEMP-190n
(INFORMAL)
Part B

INTRODUCTION TO NUCLEAR PROPULSION

Lecture 21 - NUCLEAR ROCKET SYSTEM

Russell E. Motsinger 1963

May 14, 15, and 16, 1963

Prepared for the George C. Marshall
Space Flight Center of the National
Aeronautics and Space Administration

Contract No. NAS8-5215

PREFACE

Lecture 21 has been divided into Parts A and B. Otherwise the two parts are a unit and Part B requires Part A in order to maintain proper continuity.

CONTENTS

Part B

FIGURES

Part B

TABLES

Part B

4. SYSTEM DESIGN CONSIDERATIONS

4.1 CONDITIONS IMPOSED

For sake of further discussion, assume that a reactor energy increment of 0.060 MW hr/Kg at a specific impulse of about 850 seconds performs a sufficient variety of missions to meet the goals for the near term future*. Hence, we may determine requirements that will be imposed upon the reactor, imposing conditions from Table 8:

TABLE 9
(Thermal design parametric study)

CONDITIONS IMPOSED UPON REACTOR BY TYPICAL MISSION

Shield Diameter (ft)	Flow Rate for I_{sp} = 850 sec (lb/sec)	Energy Input to Propellant (MW-hr)	Propellant Temperatures[a] (^{o}R) I_{sp}=700	850	1000sec
1	11.75	37.7	3800	4300	5500
5	411.	1320.	3800	4300	5500
10	1765.	5660.	3800	4300	5500

[a] Data for expansion ratio of 100 and chamber pressure of 1000 psi. Pressure effect becomes significant at temperatures in their range; for example, at 5500^{o}R the specific impulse varies from 985 to 1050 seconds as the chamber pressure is decreased from 4000 to 100 psia, respectively.

The characteristics of the reactor will determine which part of this range is feasible and whether there are incompatibilities in the requirements.

* See Table 5 for planets within reach with this capability; ~~also note from the lunar example included in Appendix A-1 that the Moon is included.~~

4.2 REACTOR SIZING

4.2.1 Thermal Design Requirements

The first problem in determining the feasibility of the conditions imposed upon the reactor is to establish the fuel element passage sizes. This may be done readily for initial assessment purposes by the technique developed in Appendix B-1 and data included for hydrogen in Appendix B-2, once the allowable maximum fuel element temperature and frontal area of the reactor which can be devoted to void for the coolant has been established.

Assuming that the hottest surface temperature of the average fuel element channel is to be restricted to 4860°R (4400°F) and that the hydrogen temperature upon entering the reactor inlet plenum is 200°R (higher than tank discharge temperature because of regenerative cooling of the nozzle, reflector, etc.), then Figure B1, B2, or B3 can be used for establishing the fuel element dimension parametric grouping, depending upon the shape of the longitudinal power profile. Generally the 2:1 sine curve of Figure B2 is suitable as a first approximation of actual conditions, in which case (using the nomenclature in Appendix B-2):

$$\text{Given} \quad \frac{T_{s_{max}} - T_o}{T_o - T_1} = \frac{4860 - 4300}{4300 - 200} = 0.136$$

$$\text{and} \quad \frac{T_o - T_1}{T_o} = \frac{4300 - 200}{4300} = 0.95$$

Then, from Figure B2 (Appendix B-2)

$$\frac{EL}{D_H^{1.2} G^{0.2}} = 755$$

Since the data for Figures B1, B2 and B3 are dependent upon the magnitude of temperature as well as the temperature ratios used above, the correction given in Figure B5 must be applied. In this case

$$\left(\frac{EL}{D_H^{1.2} G^{0.2}}\right)_{\text{corrected}} = 1.001 \left(\frac{EL}{D_H^{1.2} G^{.2}}\right)_{\text{uncorrected}}$$

$$= 1.001 \times 755$$

$$= 756$$

If we assume tubular fuel element channels, the value of E (ratio of passage to smooth tube heat transfer coefficient) may be taken as unity. Therefore, the temperature conditions have uniquely fixed the parametric grouping:

$$\frac{L}{D_H^{1.2}\, G^{0.2}} = 756$$

where:

L = Active (fueled) length of the fuel element channel (inches).

D_H = Hydraulic diameter (equal to hole diameter for tubular elements) of fuel element channel (inch).

G = Flow rate of coolant in channel per unit of flow area (lb/in^2 sec).

The permissible mass flow can now be found, once the pressure level and allowable pressure ratio across the reactor is known; alternately, it can be established once the permissible reactor void is known from nuclear and mechanical studies. This is so because the pressure ratio is dependent to a very close first approximation upon the parametric grouping listed above, according to:

$$\left(\frac{G\sqrt{T_1}}{P_1}\right)^2 \left(\frac{KL}{D_H^{1.2}\, G^{.2}} + \psi\right) = \xi$$

where

$\frac{G\sqrt{T_1}}{P_1}$ = A flow function, proportional to mach number, in this case defined by the inlet conditions.

ψ, ξ = Factors dependent upon pressure ratio as given in Figures B6 and B7 (Appendix B-2).

K = Ratio of actual friction factor, accounting for surface roughness and any unfueled length in the flow channel, to the continuous smooth tube friction factor.

The temperature ratio, T_o/T_i, has already been fixed, but the pressure level and pressure ratio across the reactor have not. The normal procedure is to treat these values as independent variables so that any possible optimizations may be incorporated in the design. Data in the format of Figure 9 represents typical output at this stage of the analysis, to be used in balancing requirements upon other components of the system. To gain some appreciation of feasibility of the imposed conditions, we may assume that a pressure ratio of 0.7 together with a reactor inlet pressure, P_1, of 2000 psi is tolerable and the ratio of the passage friction factor to smooth tube friction factor, K, is 1.3; then, the mass flow allowed is 1.63 lb/sec in^2, and we see from the table below that the reactor void fraction must be at least 10%, considering that the shadow shield must be larger than the active core diameter.

TABLE 10

Flow Area Required in Reactor

Shield Diameter (ft)	Flow Rate (lb/sec)	Flow Area (in^2)	Reactor Diameter (ft) for Void Fractions of 5%	10%	20%
1	11.75	7.2	1.13	.80	.57
5	411	252	6.70	4.74	3.35
10	1765	1081	13.82	9.78	6.92

Figure 9

THERMAL DESIGN, PARAMETRIC STUDY,
TYPICAL FORMAT

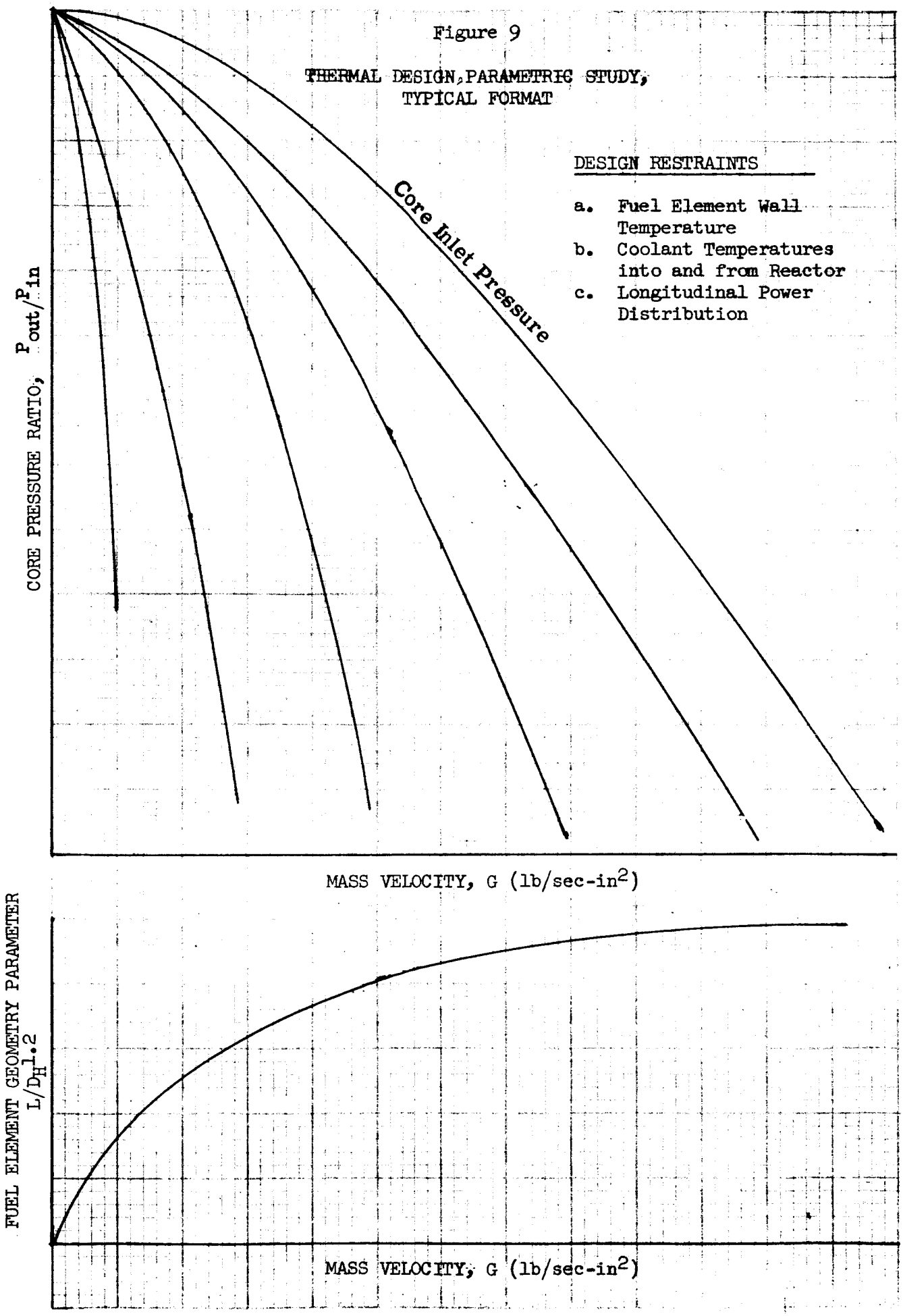

4.2.2 Nuclear Design Requirements

Nuclear analysis requires complete specification of the reactor material composition in order to determine the size necessary to achieve a critical mass with sufficient excess reactivity. In general, the fuel element temperature level necessary to achieve a gas temperature of the order of 4300°R restricts attention to refractory metals or graphite - carbide systems. Use of refractory metal implies fast-spectrum reactors because of the relatively high parasitic absorption of neutrons during slowing down to equilibrium thermal energy. On the other hand, use of graphite-carbide materials normally, though not necessarily, implies thermal reactors to take advantage of the relatively low fuel concentration required for criticality in a well moderated, low parasitic absorption system; this may be desirable for large sizes to restrict the weight and fuel inventory of the system.

Cooper reports* that tungsten, the most promising refractory metal candidate, is neutral in its effect upon reactivity in a fast-spectrum reator; consequently, it is neutral upon reactor core size so long as the amount of fuel is held constant. Hence, tungsten or void have essentially identical effects upon core size. (This conclusion applies for the range investigated which was 15 to 40 volume percent UO_2 and 25 to 60 volume percent tungsten in the reactor.) Provided data for critical masses of U235 fuel therefore, a first approximation of the size of the reactor can be obtained as a function of various void and tungsten volume fractions. A method for accounting for the introduction of voids and for converting from spherical to cylindrical geometry is included in Appendix B-3, the derivation shows that:

$$r_V = \frac{r}{S} = \frac{r}{(1 - V)}$$

and $$M_V = \frac{M}{(1 - V)^2}$$

where: r, M = critical radius and critical mass of the solid reactor (without voids or equivalent diluents)

r_V, M_V = radius and mass with voids

S = volume fraction of the solid material

V = void fraction.

* LA-2707, 'Fast Reactor Rocket Engines - Criticality," Ralph S. Cooper, Oct. 15, 1962.

In the case of the fast-spectrum reactor, S should be interpreted as the volume fraction of fuel, and V should be interpreted as the remainder of the core volume devoted to void and tungsten. Cooper reports data* as given in Figure 10 for a spherical core reflected with 12 cm of beryllium 75% of theoretical density which is in substantial agreement with similar analyses done at GE-NMPO; extrapolation of Cooper's data by the above formula for r_V appears to be suitable for feasibility studies of interest here. Since these data are for spherical geometry, modification to cylindrical geometry is required. Conversion formulae listed in Appendix B-3 for core length-to-diameter ratios of 1.0, 1.5, and 2.0 can be applied once the extrapolation distance, d = [redacted] $0.7/\Sigma$ (See GEMP-190c), is known. For use in design, the fraction of tungsten filler in the form of carrier of the UO_2 fuel and in the form of cladding for retaining fission products must be determined so that the size required to permit the necessary flow area can be fixed. An example of the format of typical output of parametric nuclear sizing data for cylindrical geometry cores, including tungsten carrier for the UO_2 in the form of cladding and dilvent in the W-UO_2 matrix is shown in Figure 11. It should be noted that the nuclear data presented in Figure 10 are subject to modification depending upon the results of critical experiments; but are reasonably representative of analytical results to be expected for fast-spectrum, refractory metal reactors. For the ratio of core length-to-diameter, L/D, equal to 1, the relationship of diameter to free flow area for a core carrying the proper amount of tungsten is closely approximated by:

$$D = 4.43 + 1/2 \sqrt{78.5 + 9.68\, A_{ff}}$$

where D = core diameter (inches)

A_{ff} = free flow area (sq. inches)

* Ibid.

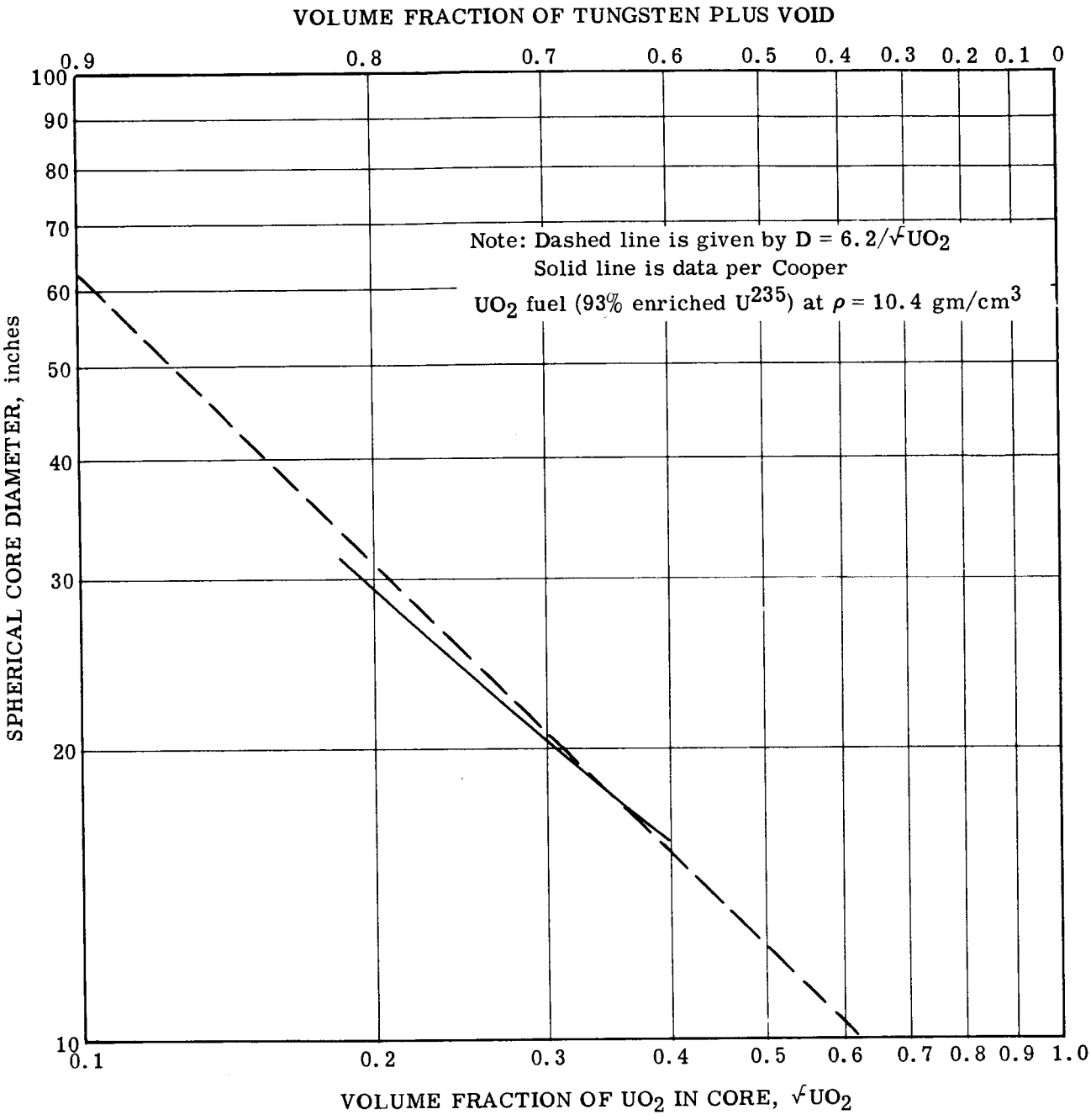

Fig. 10 - Critical diameter of UO_2-W core reflected by 12 cm of Be at 75% theoretical density (per Cooper, LA-2707)

Figure 11

Typical Format for Size of Cylindrical Reactors
with Engineered Structural Content

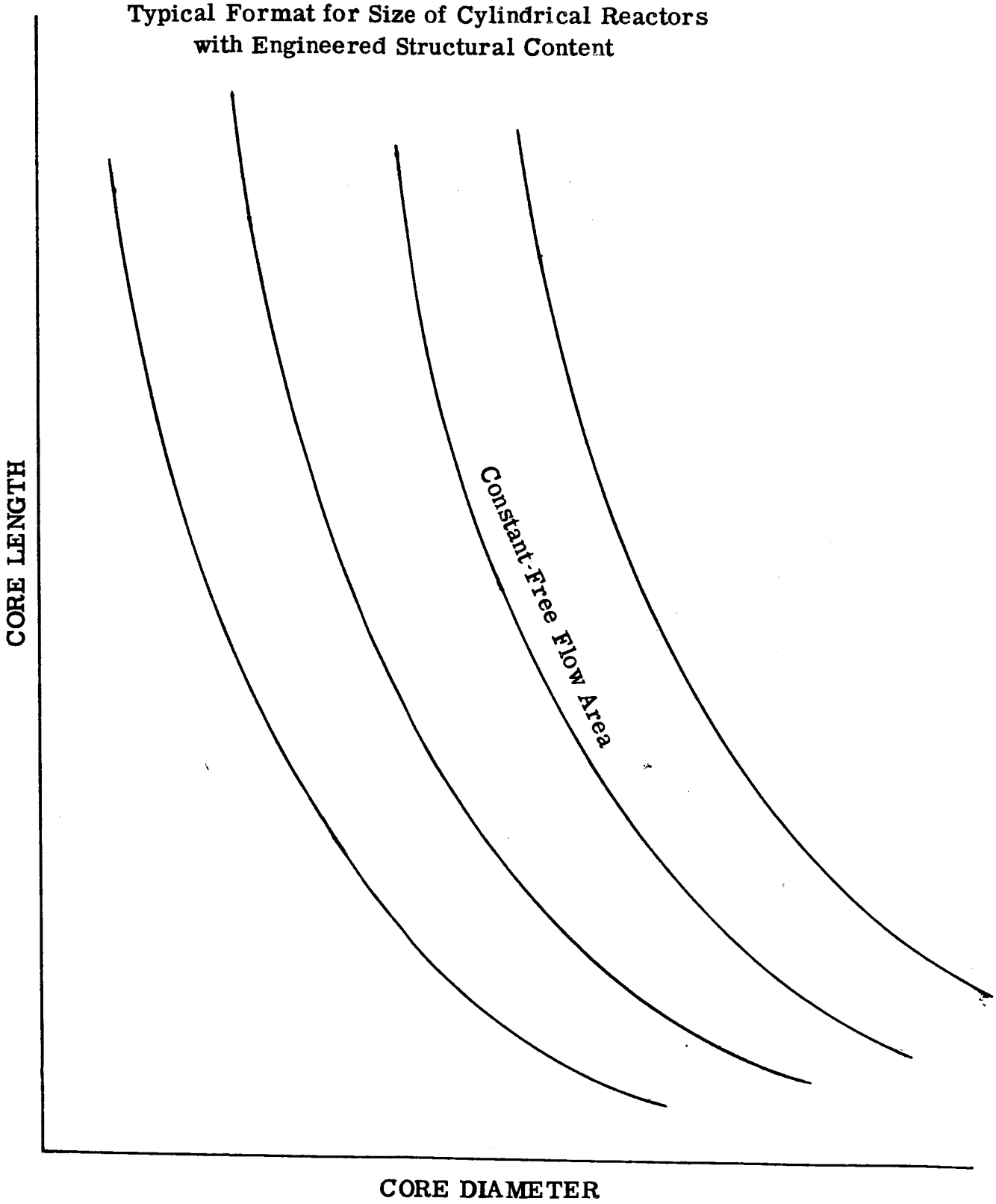

Hence, the feasibility of achieving the required thrust for the conditions imposed in par. 4.1 and the free flow areas of par. 4.2.1 is shown by:

TABLE 11

Critical Reactor Diameter for Imposed Conditions

Shield Diameter (ft)	Flow Area (in^2)	Critical Reactor Diameter (ft)
1	7.2	0.875
5	252	2.46
10	1081	4.64

This shows that the fast-spectrum reactor can provide sufficient thrust to boost the non-propellant weight implied by the initial assumption that the shield weight is 25% of the burnout weight. The actual shield weight fraction of the amount weight depends upon the shadow angle that must be shielded.

There will be some upper limit on size placed upon fast reactors because of the high fuel inventory required; some appreciation of this can be seen by using Figure 10 to estimate the amount of UO_2 in the cores sized so far:

TABLE 12

Fuel Investment (lb UO_2) in Spherical Reactor

Core Diameter (ft)	Volume Fraction of UO_2 (ρ = 10.4)	Weight of UO_2 (lb)
0.875	0.60	137
2.46	0.21	1050
4.64	0.112	3810

These data are approximate, involving large extrapolations of Cooper's data at either extreme, but reasonably shows the trend. There is no hard and firm rule for drawing a line, but the cut-off point must be made after performing good engineering design and comparing the results with similarly valid designs of alternate materials.

The data in Appendix B-3 for U235-Carbon bare sperical critical reactors illustrates how use of moderation can reduce the critical mass as the size of the core increases. No attempt will be made here to make a comparitive study because a wealth of information already exists on designs of systems using graphite, and the reader is cautioned to be very wary of any attempts at generalization with thermal reactors when complete specification of all structural material compositions and volume fractions is not given. Since hydrogen reacts with carbon at temperatures necessary for rockets, a protective cladding must be included; the cladding may act as a significant poison and achieving the potential savings in fuel investment promised by moderation may be difficult. Despite this possible difficulty, the fact remains that graphite density is about one order magnitude lower than that of tungsten, and if the weight of the reactor, itself, is important in the thrust-to-weight ratio for the entire engine, significant benefit in the larger size range may accrue.

4.3 NON-REACTOR ENGINE COMPONENTS

The overall weight of the engine can be minimized by making a proper balance of the weight of individual components as they vary with pressure level of the hydrogen. For example, the reactor size will decrease as the pump discharge pressure is increased or as the pressure loss across the fuel elements is increased. The exhaust nozzle will decrease in weight as the pump discharge pressure increases, but will increase in weight as the reactor pressure loss increases. Pump weight obviously increases as the discharge pressure increases.

The data presented in Section 4.2 is sufficient for estimating reactor core weights, assuming the refractory metal as the reactor material, as a function of pressure level and pressure loss for the imposed conditions. Shadow shield weight can be determined from the core size data, once a suitable shadow angle has been determined considering suitable tank proportions and either separation distances between reactor and tank or between reactor and payload.

Typical data for the nozzle weight are given in Figure 12. This plot shows weight as a function of pressure shell diameter, throat diameter, and chamber pressure level for a regeneratively cooled nozzle with an expansion ratio of 40.

Fig. 12
TYPICAL DATA FOR
NOZZLE WEIGHT vs. PRESS. SHELL DIA.

For:

Throat Dia. - 4.0 to 12.0 in.
Chamber press. - 500 to 2000 psia
Max. Allow. stress - 60000 psi
Density - 484 lb/ft^3
Conv. Half-angle - 45°
Divergent Half-angle - 15°
Area Ratio - 40
Regenerative cooled
per NASA TN-D-675

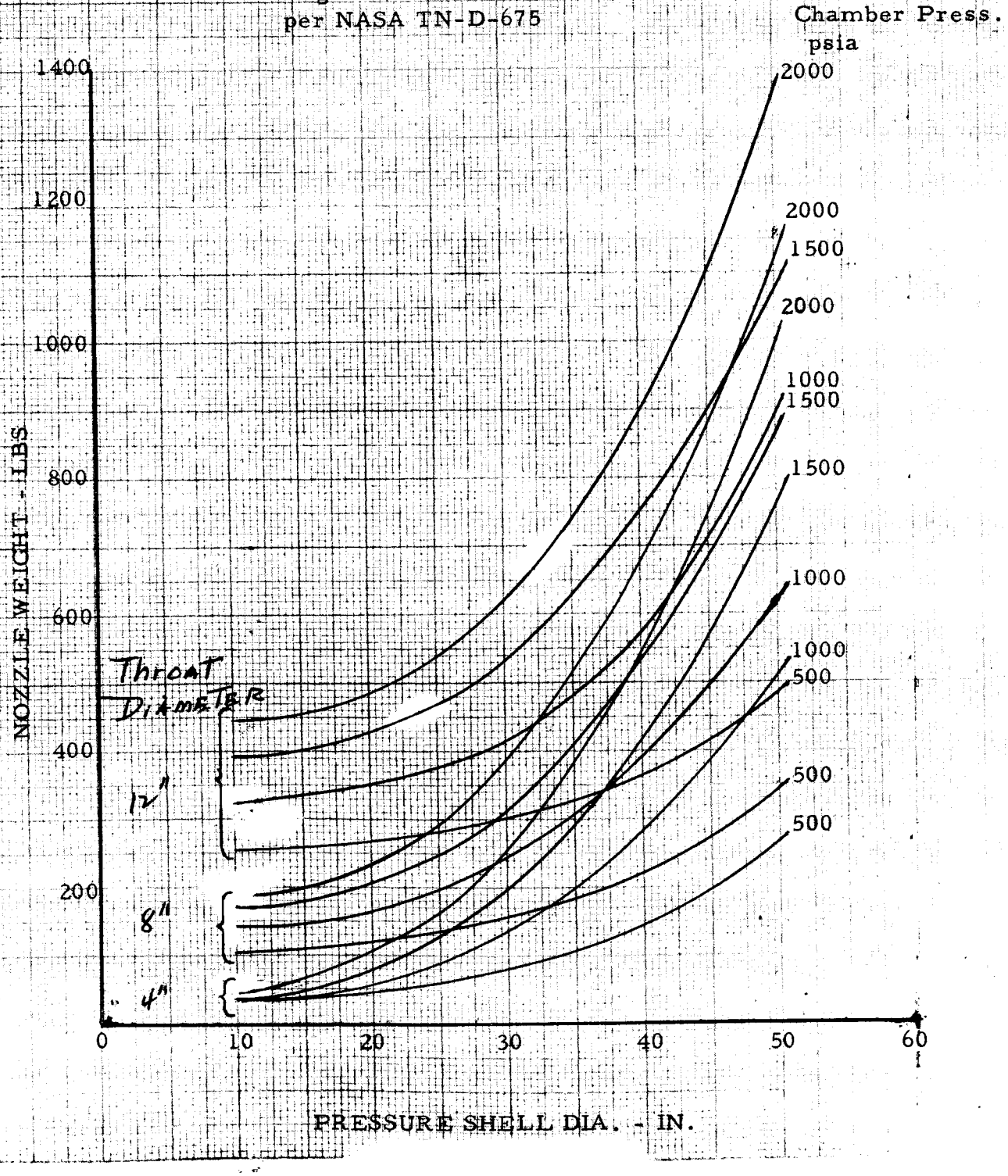

Data for the weight of the pump are given in Figure 13. This data assumes weight is directly proportional to flow rate and pressure level.

The combination of these effects results in curves such as given in Figure 14 for an unshielded case. The curves show minimum engine weights occur at chamber pressures between 1000 and 2000 psi and as the pressure loss is increased from 200 to 1000 psi the weight is continually reduced. Such data are highly dependent upon the structural design incorporated in the reactor.

4.4 DISCUSSION

The results of the first appraisal of the implications of the conditions which have been imposed to this point are given in Table 13. One measure of feasibility of the assumed conditions is shown by the values of dry vehicle weight, W_f (which is a direct result of the assumed values of initial vehicle weight, W_o, the specific impulse, and the propellant energy increment) and the total engine and tank weight (which is a calculated result based upon the weights of individual components necessary to perform the function required of them). Another measure is the size of the active core relative to the assumed shield diameter; this is of particular importance insofar as it is a measure of the shadow angle given by the shield.

Both these factors show that the smallest size vehicle in the comparison does not meet the requirements because: (a) the total engine and tank weight of 1530 lb is greater than the allowed value of 1,390 lb given by the dry vehicle weight, and (b) the reactor diameter, 0.88 ft, is nearly equal to the shield diameter of 1.0 ft, so the shadow angle is very small.

The two larger sizes indicate the feasibility of achieving the assumed thrust (i.e. a thrust-to-weight ratio of 1) within the dry vehicle weight limitation if a tank weight fraction equal to 5% of the propellant weight is possible; were that fraction to be higher, the payload fraction would be essentially zero for the cone angle which is shielded. The active core diameter for each of the larger reactors is less than one-half the assumed shadow shield diameter. Since the shield weight fraction is large for the conditions assumed, properly sizing the shield while all other factors are held constant will yield significant benefit in trade-off studies among shield, tank, and payload weight.

The largest size vehicle is probably at the boundary dividing the choice between use of a fast-spectrum or a moderated epithermal or thermal-spectrum reactor material because of the relatively high investment of fuel required for criticality in such a large size system. However, it is

Fig. 13 - Typical Data for Weight of Pump

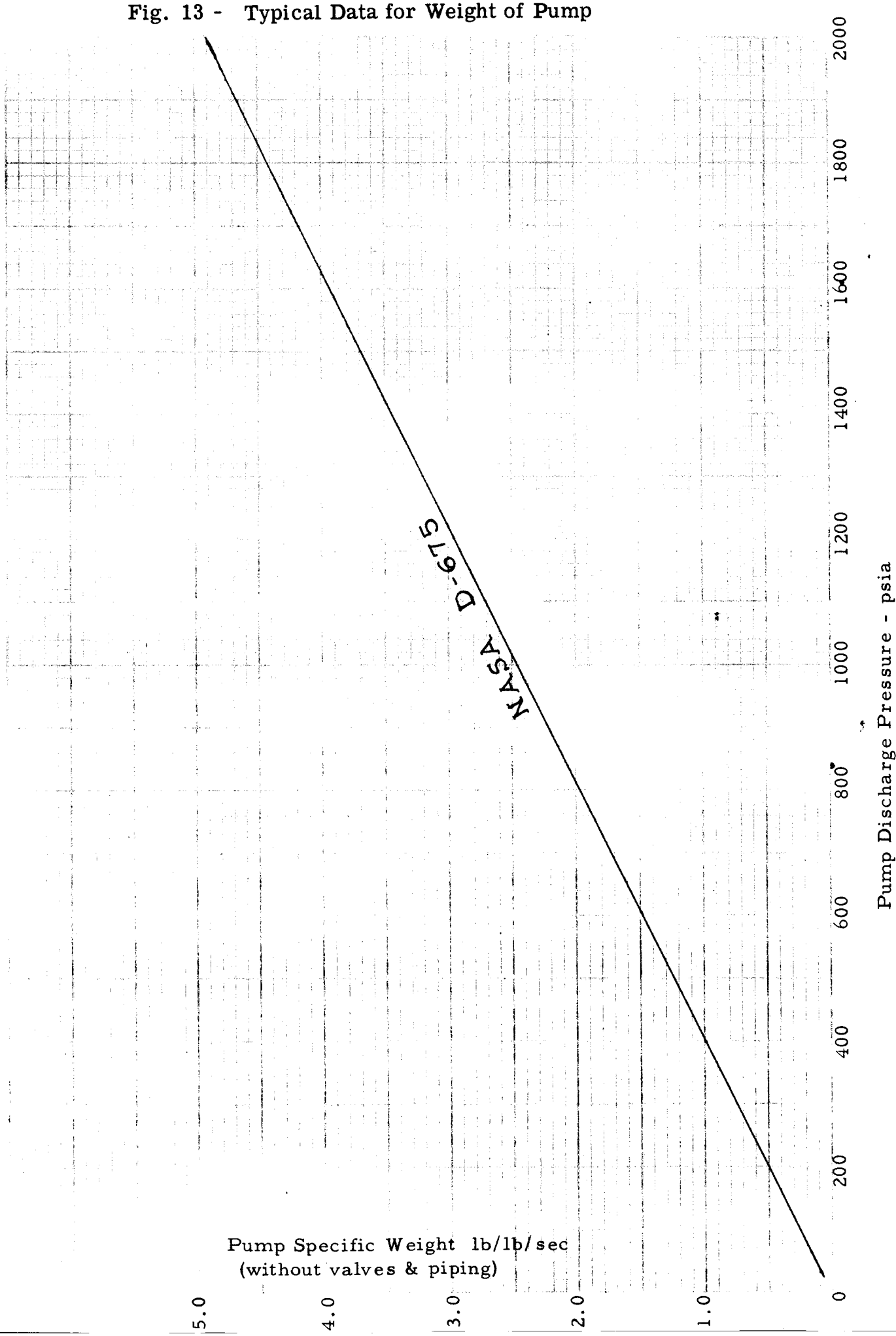

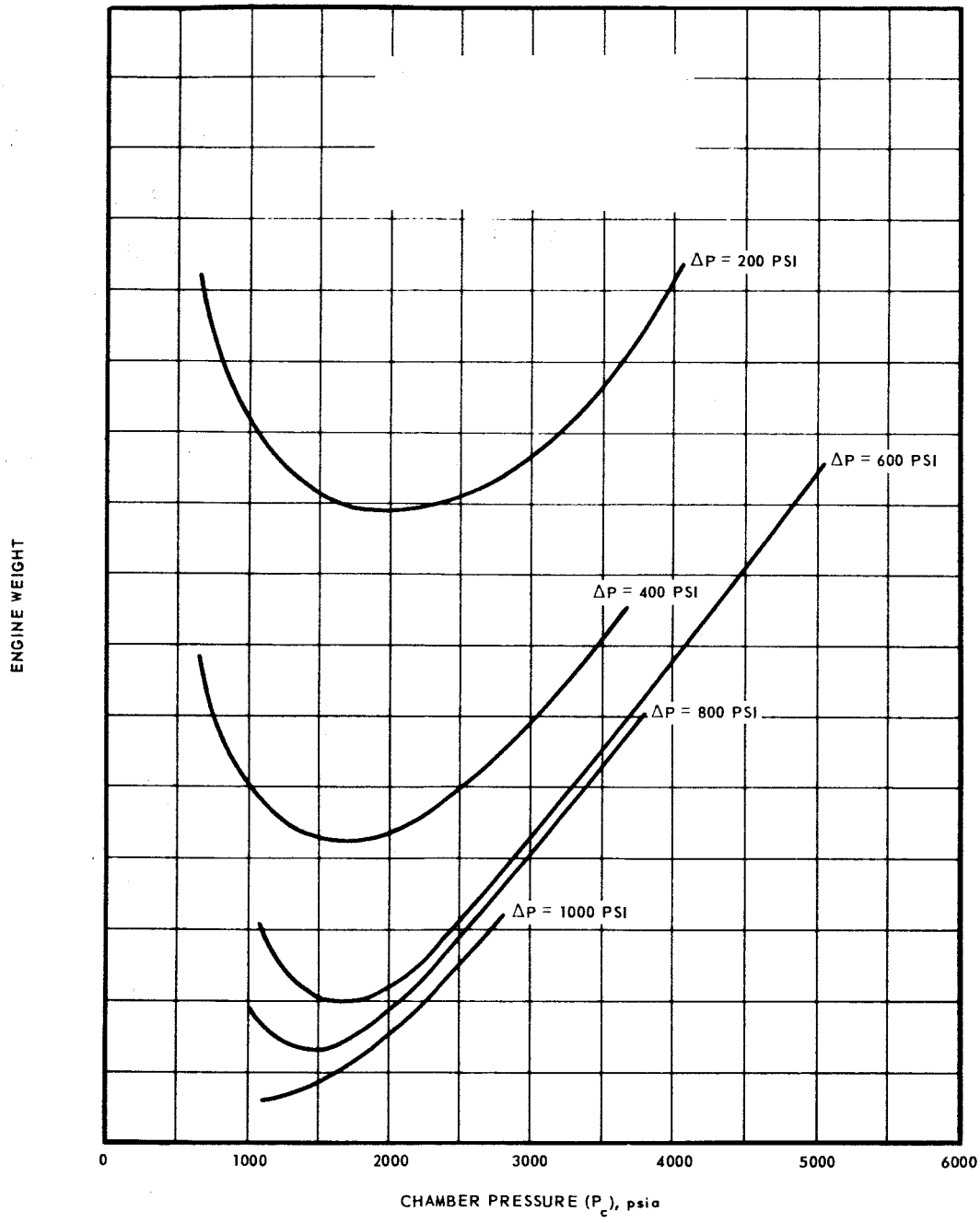

Fig. 14 - Typical weight optimization curves to select reactor core pressure level and pressure drop

TABLE 13

Survey of Results for Imposed and Assumed Conditions

Imposed Conditions

Shield Diameter (ft)	1	5	10
Initial Vehicle Weight, W_o (lb)	10,000	350,000	1,500,000
Engine Thrust, F_v (lb)	10,000	350,000	1,500,000
Specific Impulse, I_{sp} (sec)	850	850	850
Propellant Energy Increment, $\frac{Q}{W_f}\left(\frac{\text{MW hr}}{\text{Kg}}\right)$	0.060	0.060	0.060

Assumed Conditions

Propellant	Hydrogen
Materials	
Reactor Core	Tungsten - UO_2 (93.2% U^{235}, ρ = 10.4 gm/cm^3)
Reflector	Beryllium
Shadow Shield	Iron
Pressure at Reactor Inlet	2000 psia
Pressure Ratio Across Reactor	0.70

Derived Conditions

Propellant Weight, W_p (lb)	8,610	301,500	1,292,000
Dry Vehicle Weight, W_f (lb)	1,390	48,500	208,000
Propellant Temperature (^oR)	~4,300	~4,300	~4,300
Propellant Flow Rate, W_p (lb/sec)	11.75	411	1,765
Burn Time, t_B (sec)	733	733	733
Propellant Energy Increment (MW hr)	37.7	1,320	5,660
Power to Propellant (MW)	185	6,500	27,800
Power Density* (MW/ft^3)	350	560	360
Reactor Core Flow Area, A_{ff} (in^2)	7.2	252	1,081
Reactor Diameter, $D_c = L_c$ (ft)	0.88	2.46	4.64
Fuel Inventory, (lb UO_2)	~200	~1,600	~5,700
Reactor Weight (lb)	~550	~8,000	~48,000
Shadow Shield Weight (lb)	450	15,400	68,600
Nozzle Weight (lb)	~40	~600	~2,000
Pump Weight (lb)	~60	~2,100	~9,000
Tank Weight @ 5% W_p, (lb)	430	15,000	64,600
Total Engine and Tank Weight (lb)	1,530	41,100	192,200

* Per unit volume of active core.

possible that operational considerations such as restart capability yielding the possibility of multiple reuse, or engine reliability inherent in clusters of smaller engines, may modify any conclusions which might be drawn on the basis of single-use missions.

The power densities in all three cases are extremely high compared with earth based nuclear reactors, being in the vicinity of 100 to 200 times as great. Consequently, it is imperative to have a large number of cooling channels so as to include a large surface-to-volume ratio for heat removal from the active core, thereby minimizing internal temperature gradients and thermal stresses. Proof of structural designs subject to high thermal stresses depends upon demonstration in full power tests of the actual reactor design since power densities such as required in the rocket application cannot be duplicated in component tests by other means.

5. SUMMARY

This is the last lecture of the series, and it would be fitting to summarize here all the pertinent facets discussed by the various contributors. Suffice it to say, rather, that many varied skills and technologies must be brought together in a high degree of sophistication to achieve the necessary levels of safety, reliability, performance, operational capability, and timeliness of schedules. It is hoped that the series has served to indicate not only most of the significant problems that must be anticipated but also some reasonable indication of the best technical approach for solving these problems.

The present lecture has been aimed at giving some feeling for the possible capability of nuclear rockets, regimes in which it should or should not be considered based upon expected capability in the near term future, and, for those who wish to make ballpark checks of design results or feasibility of new missions, some indication of the tools of the trade. There are many other items that logically should have been included in this discussion, but those must be reserved until the ability to state things more concisely is gained with increased engineering experience in the field of nuclear rockets. An indication of the start that has been made towards making engineering designs of nuclear rockets is given by the illustrations shown in Figures 15 and 16. Details of these nuclear rocket engine designs may be obtained from the reports of the appropriate government agencies and contractors.

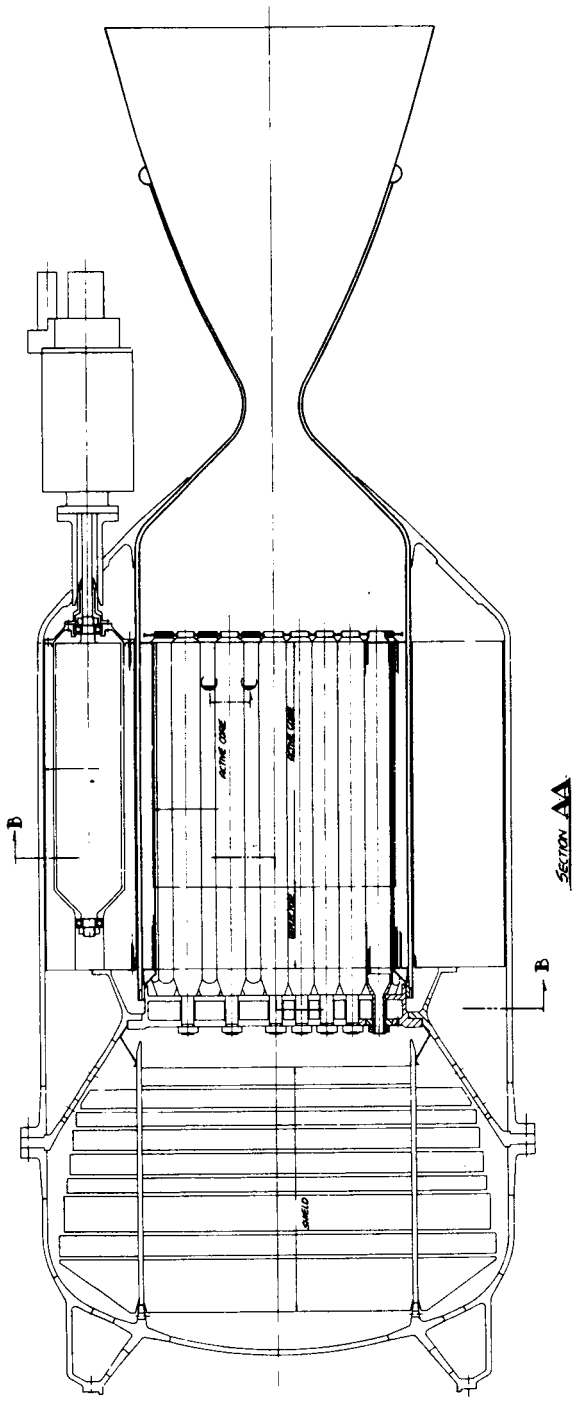

Fig. 15 - A Typical Rocket Engine Configuration

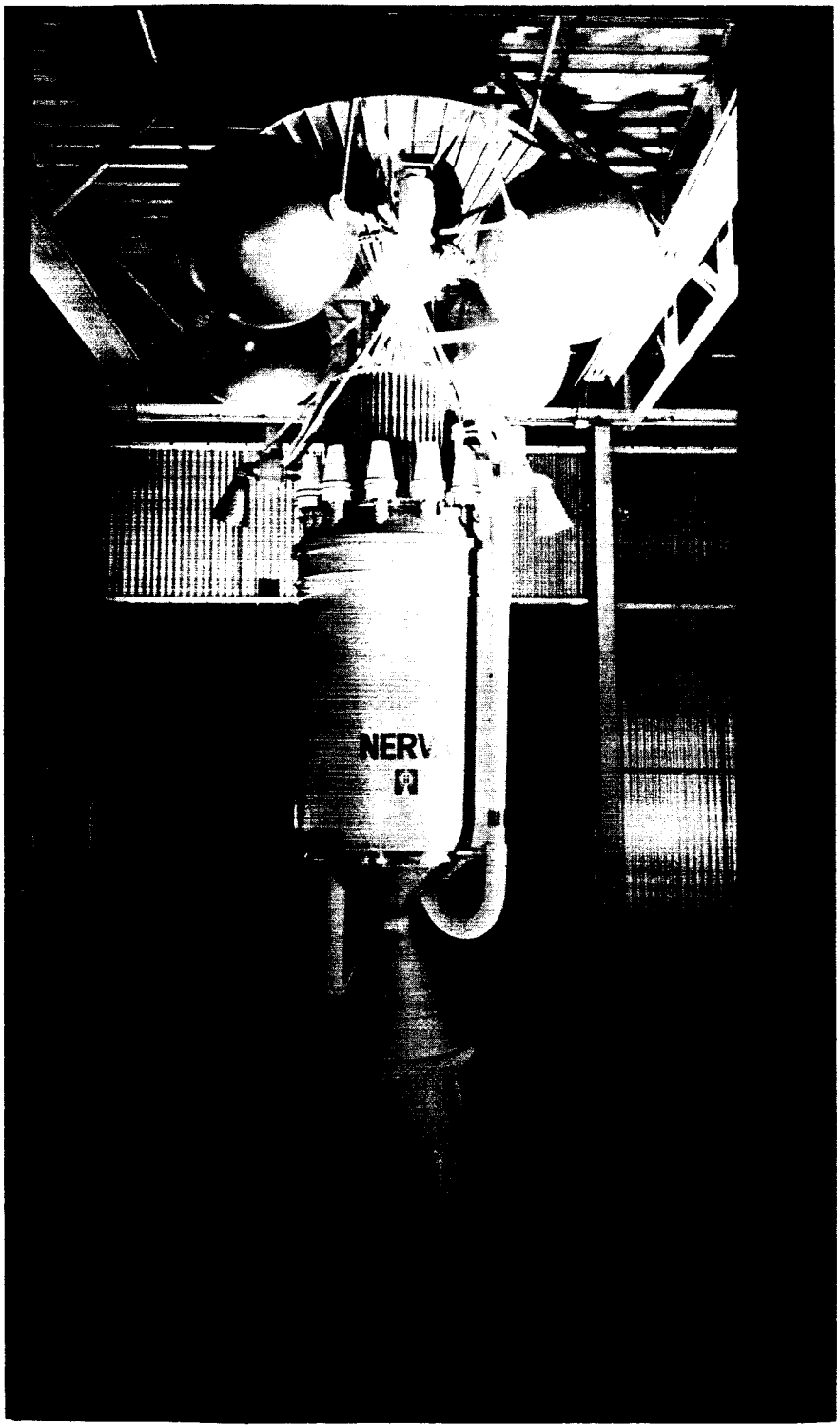

Fig. 16 - Mockup of NERVA Nuclear Rocket Engine

APPENDIX B-1*

1. THERMODYNAMICS OF FUEL ELEMENTS

This presentation is formulated for the case of turbulent air in conduit-type passages, as in tubular systems or plate-type elements, but the same type of presentation can be developed either for other coolants or for other fuel element types.

1.1 Short-Form Temperature Calculation

Experience with the use of this method has shown that the accuracy of temperature estimates is within ±5 percent of that obtained by incremental solutions from computers.[1]

Use of this method is possible because a parameter fixed only by the fuel element geometry and coolant mass flow rate is related to a parameter fixed only by the coolant temperatures at the entrance and discharge of the reactor and by the maximum fuel element temperature required to achieve the required coolant temperature:

$$\frac{EL}{D_H^{1.2}\, G^{0.2}} = f\,\frac{T_{s_{max}} - T_3}{T_3 - T_2} \tag{98}$$

where

- E = ratio of the actual heat transfer coefficient to the smooth-tube heat transfer coefficient, $c = 0.0205$, in the equation $N_u = c\, N_R^{0.8} N_{pr}^{0.4}$
- L = active length of the fuel element
- D_H = hydraulic diameter of the coolant channel
- G = coolant mass flow rate
- $T_{s_{max}}$ = maximum surface temperature of the average fuel element, wherever it occurs in the longitudinal direction (direction of flow)
- T_3 = reactor coolant discharge temperature
- T_2 = reactor coolant inlet temperature

The term $EL/D_H^{1.2}\, G^{0.2}$ is the identical parameter needed to fix the pressure ratio.

In an open cycle reactor, heat addition is by convection of the heat generated in the fuel elements to the air stream as it flows through the active core. Reactor size, therefore, depends as much on the dimensions of the coolant passages as on the mass of solid material. The total area of a reactor core A_c can be expressed in terms of the total passage or free flow area A_{ff} by employing a factor called the free flow fraction R_{ff}:

$$A_c = \frac{A_{ff}}{R_{ff}} \tag{99}$$

The free flow fraction is determined by the configuration of the reactor and the materials of which it is fabricated. The passage dimensions are functionally related to the power distribution in the reactor and to the air properties at the core inlet and discharge.

* Note: This material is abstracted from APEX-800, Part A.

For configurations having constant area coolant passages, the passage area and length can be calculated using equations derived from aerothermal relationships for heat addition to air flowing in constant area ducts.

Equations (100) through (137) relate fuel element temperature to required operating temperatures, T_2 and T_3, and to the fuel element geometry characteristics. Plots and nomograms for appropriate equations are given in reference 1.

The relationship

$$q = h A_h \Delta T \tag{100}$$

where h is the coefficient of heat transfer is applied to the heat transferred from the reactor passage surface to the coolant gas across an increment of passage wall dx. The rate of heat transferred per unit of passage wall area is related to the passage surface temperature, T_{sx}, and the mixed mean temperature of the gas T_x by:

$$\frac{dq_x}{d(A_h)_x} = h(T_{sx} - T_x) \tag{101}$$

Assuming that there is no heat conduction within the solid which is parallel to the passage, dq_x is also the rate of heat generated in a volume $A\,d_x$, where A is the fuel area associated with and normal to the passage. The volumetric heat source, or reactor power density, is a point function, but a local average power density Q'_x at dx can be defined:

$$dq_x = A\,Q'_x\,dx \tag{102}$$

If p is the coolant passage perimeter, then:

$$d(A_h)_x = p\,dx \tag{103}$$

When the expressions in Equations (102) and (103) are substituted for dq_x and $d(A_h)_x$ in Equation (101), the local temperature differential across the solid-coolant convective resistance can be expressed in terms of the local average power density as follows:

$$T_{sx} - T_x = \frac{A\,Q'_x}{hp} \tag{104}$$

Average power density varies along the length of the core. In a uniform bare cylinder or rectangular parallel-piped reactor, the neutron flux and power density may be approximated by a sine distribution in the longitudinal direction of the form:

$$Q'_x = Q'_{max} \sin \frac{\pi x}{L_c} \tag{105}$$

In the practical case, the core will have both radial and end reflectors, and Equation (105) becomes:

$$Q'_x = Q'_{max} \sin \frac{\pi}{s}\left(\frac{x}{L_c} + a\right) \tag{106}$$

where a is a measure of the thickness of the front reflector and x = 0 at the inlet to the reactor core, as shown in Figure 2.3-1.

When Equation (106) is substituted into Equation (104), the relationship becomes:

$$T_{sx} - T_x = \frac{Q'_{max}\,A}{hp} \sin \frac{\pi}{s}\left(\frac{x}{L_c} + a\right) \tag{107}$$

Since values of T_x are known only at core inlet and discharge, the general term for coolant temperature T_x in Equation (107) must be replaced by an equivalent expression in terms of known parameters.

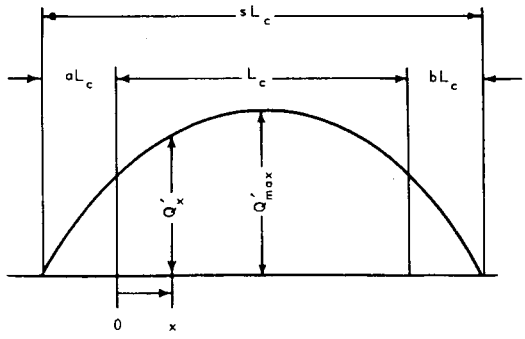

Fig. 2.3-1 – Reactor power distribution curve

The rate at which heat is added to the gas in a differential length dx of any coolant passage is:

$$dq_x = W C_p \, dT \tag{108}$$

where W = gas flow through the passage
C_p = specific heat

When Equation (102) is substituted for dq_x, the integral form of Equation (108) for the steady flow in the constant area passages from the core inlet, state 2, to any point x is:

$$\int_{T_2}^{T_x} dT = \frac{A}{W C_p} \int_0^x Q'_x \, dx \tag{109}$$

If the local average power density, Q'_x, is replaced by its equivalent expression from Equation (106), the integration can be completed to give the differential in the mixed mean temperature of the coolant gas:

$$T_x - T_2 = \frac{Q'_{max} A L_c}{W C_p} \left(\frac{s}{\pi}\right) \left[\cos \frac{\pi a}{s} - \cos \frac{\pi}{s} \left(\frac{x}{L_c} + a\right)\right] \tag{110}$$

If the integration of Equation (109) is performed over the entire core length, from state 2 to state 3 and the integral of $Q'_x \, dx$ from 0 to L_c is $Q'_{avg} L_c$, the following is obtained:

$$A L_c Q'_{avg} = W C_p (T_3 - T_2) \tag{111}$$

When the ratio of maximum to average power density is expressed as Ψ_{max}, the substitution of Equation (111) into Equation (110) yields:

$$T_x - T_2 = \Psi_{max} (T_3 - T_2) \left(\frac{s}{\pi}\right) \left[\cos \frac{\pi a}{s} - \cos \frac{\pi}{s} \left(\frac{x}{L_c} + a\right)\right] \tag{112}$$

Use of the definition of Ψ_{max} and the equivalence of $p L_c$ to A_h, the combination of Equations (111) and (107) produces:

$$T_{sx} - T_x = \Psi_{max} (T_3 - T_2) \frac{W C_p}{h A_h} \sin \frac{\pi}{s} \left(\frac{x}{L_c} + a\right) \tag{113}$$

The general term for coolant gas temperature T_x can be eliminated by adding Equations (112) and (113):

$$T_{sx} - T_2 = \Psi_{max} (T_3 - T_2) \left\{\left(\frac{S}{\pi}\right)\left[\cos \frac{\pi a}{s} - \cos \frac{\pi}{s} \left(\frac{x}{L_c} + a\right)\right] + \frac{W C_p}{h A_h} \sin \frac{\pi}{s} \left(\frac{x}{L_c} + a\right)\right\} \tag{114}$$

Before the size of the coolant passages can be determined, the location at which T_{sx} attains a maximum value must be ascertained. This is accomplished by differentiating Equation (114) and setting the result equal to zero:

$$\tan\theta = -\left(\frac{\pi}{s}\right)\frac{W C_p}{h A_h} \tag{115}$$

where

$$\theta = \frac{\pi}{s}\left(\frac{x}{L_c} + a\right)$$

The geometrical dimensions of the coolant passages are derived from the heat transfer coefficient. Assuming that Equation (115) defines the location of $T_{s_{max}}$, the substitution of the expression for this location into Equation (114) yields a relationship between known temperatures, reactor power distribution, and the heat transfer coefficient:

$$\frac{T_{s_{max}} - T_2}{T_3 - T_2} = \Psi_{max}\left(\frac{s}{\pi}\right)\left(\cos\frac{\pi a}{s} - \frac{1}{\cos\theta}\right) \tag{116}$$

or:

$$\frac{1}{\cos\theta} = \cos\frac{\pi a}{s} - \left(\frac{T_{s_{max}} - T_2}{T_3 - T_2}\right)\left(\frac{\pi}{s}\right)\left(\frac{1}{\Psi_{max}}\right) \tag{117}$$

The maximum-to-average power-density ratio Ψ_{max} can be expressed in terms of a, b, and s by integrating Equation (106) between 0 and L_c:

$$\Psi_{max} = \left(\frac{\pi}{s}\right)\frac{1}{\cos\left(\frac{\pi a}{s}\right) + \cos\left(\frac{\pi b}{s}\right)} \tag{118}$$

Substituting Equation (118) into Equation (117) results in:

$$\frac{1}{\cos\theta} = \cos\left(\frac{\pi a}{s}\right) - \left(\frac{T_{s_{max}} - T_2}{T_3 - T_2}\right)\left(\cos\frac{\pi a}{s} + \cos\frac{\pi b}{s}\right) \tag{119}$$

The parameter α, defined as $-1/\cos\theta$, can be written:

$$\alpha = \left(\frac{T_{s_{max}} - T_3}{T_3 - T_2}\right)\cos\frac{\pi a}{s} + \left(\frac{T_{s_{max}} - T_3}{T_3 - T_2} + 1\right)\cos\frac{\pi b}{s} \tag{120}$$

For trigonometric identities,

$$\tan\theta = -\sqrt{\alpha^2 - 1} \tag{121}$$

Therefore, Equation (115) can be written:

$$\frac{h A_h}{W C_p} = \left(\frac{\pi}{s}\right)\left(\frac{1}{\sqrt{\alpha^2 - 1}}\right) \tag{122}$$

Examination of Equations (120) and (122) shows that the parameter $(h A_h/W C_p)$ is defined solely by terminal temperatures and power distributions.

For turbulent flow of air in conduits, the heat transfer coefficient, using units of inches, seconds, ^{o}R, Btu, lb_f, h can be expressed as

$$h = (8.44)\,(10^{-5})\,E\left(\frac{G^{0.8}}{D_H^{0.2}}\right)\frac{(T_{bm})^{0.8}}{(T_f)^{0.56}} \tag{123}$$

From the definition of the hydraulic diameter of a flow passage, the heat transfer area can be expressed as

$$A_h = 4 A_{ff}\frac{L_c}{D_H} \tag{124}$$

The specific heat at constant pressure can be approximated by

$$C_p \cong 0.103\ T_{bm}^{0.13} \tag{125}$$

Combining Equations (122) through (125) to eliminate the term (hA_h/WC_p), the geometry requirements to produce a stated value of $T_{s_{max}}$ with a particular power distribution and values of T_3 and T_2 given are defined by:

$$\frac{hA_h}{WC_p} = \frac{\pi}{s}\ \frac{1}{\sqrt{\alpha^2 - 1}} = (3.278)\ (10^{-3})\ E \left(\frac{L_c}{D_H^{1.2} G^{0.2}}\right)\left(\frac{T_{bm}^{0.67}}{T_f^{0.56}}\right) \tag{126}$$

An expression for T_{bm} can be obtained from Equation (113) when x equals that value at which $T_{s_{max}}$ occurs:

$$T_{s_{max}} - T_{bm} = \frac{\Psi_{max} \sin\theta}{\frac{hA_h}{WC_p}} (T_3 - T_2) \tag{127}$$

When Equations (118) and (120), are combined, Ψ_{max} can be written as follows:

$$\Psi_{max} = \frac{\frac{\pi}{s}}{\alpha - \cos\left(\frac{\pi b}{s}\right)} \left(\frac{T_{s_{max}} - T_3}{T_3 - T_2}\right) \tag{128}$$

From the definition of α, in Equation (120),

$$\sin\theta = \left(\frac{1}{\alpha}\right)\ \sqrt{\alpha^2 - 1} \tag{129}$$

Substituting for the parameters in Equation (127) the appropriate expressions from Equations (122), (128), and (129), the value of T_{bm} is defined by:

$$\frac{T_{s_{max}} - T_{bm}}{T_{s_{max}} - T_3} = \frac{\alpha^2 - 1}{\alpha^2 - \alpha \cos\left(\frac{\pi b}{s}\right)} \tag{130}$$

The average film temperature, $T_f = (T_{s_{max}} + T_{bm})/2$; and Equation (130) can be written:

$$\frac{T_{bm}^{0.67}}{T_f^{0.56}} = T_{s_{max}}^{0.11} \frac{\left[1 - \left(\frac{T_{s_{max}} - T_3}{T_{s_{max}}}\right)\left(\frac{\alpha^2 - 1}{\alpha^2 - \alpha \cos\left(\frac{\pi b}{s}\right)}\right)\right]^{0.67}}{\left[1 - \frac{1}{2}\left(\frac{T_{s_{max}} - T_3}{T_{s_{max}}}\right)\left(\frac{\alpha^2 - 1}{\alpha^2 - \alpha \cos\left(\frac{\pi b}{s}\right)}\right)\right]^{0.56}} \tag{131}$$

Equation (126) can be solved for the term involving coolant passage dimensions, $L_c\ D_H^{1.2} G^{0.2}$. Before proceeding to the reactor pressure drop analysis which allows the determination of the individual dimensions, the limits of applicability of the thermal design equations must be investigated.

As mentioned previously, Equation (115) defines the location at which T_{sx} attains a maximum value. In some cases, the mathematical location may be outside the reactor core, i.e., $x > L_c$. Since this is physically impossible, $T_{s_{max}}$ will have the highest value of T_{sx} within the core, which is that value occurring at core discharge, state 3. The thermal design relationships shown in Equations (120), (126), and (131) were derived on the basis of $T_{s_{max}}$ being a mathematical maximum at the location specified by

Equation (115). When the location of $T_{s_{max}}$ is core discharge, the thermal design relationships can be derived more simply from the basic heat transfer equations.

The surface-to-coolant temperature differential at core discharge, x = L, for $T_{s_{max}}$ occurring at state 3 can be determined from the convective heat transfer Equation (104). As mentioned previously, p L_c is equivalent to A_h. When both numerator and denominator of Equation (104) are multiplied by L_c, the equation becomes:

$$T_{s_{max}} - T_3 = \frac{A\ L_c\ Q'_L}{h\ A_h} \tag{132}$$

Similarly, heat transfer Equation (111) is applicable to this case. The form Q'_L must be related to Q'_{avg} in terms of known variables. When x = L, the power distribution equation, previously Equation (106), is:

$$Q'_L = Q'_{max} \sin\left(\frac{\pi b}{s}\right) \tag{133}$$

In Equation (118), Ψ_{max} is defined as the ratio of maximum-to-average power density. Therefore, by multiplying Equations (118) and (133), the required relationship between Q'_L and Q'_{avg} is determined:

$$\frac{Q'_L}{Q'_{av}} = \left(\frac{\pi}{s}\right) \frac{\sin\left(\frac{\pi b}{s}\right)}{\cos\left(\frac{\pi a}{s}\right) + \cos\left(\frac{\pi b}{s}\right)} \tag{134}$$

Combining Equations (111), (132), and (134), the quantity $(h\,A_h/W\,C_p)$ for the limiting condition can be expressed:

$$\frac{h\,A_h}{W\,C_p} = \left(\frac{T_3 - T_2}{T_{s_{max}} - T_3}\right)\left(\frac{\pi}{s}\right) \frac{\sin\left(\frac{\pi b}{s}\right)}{\cos\left(\frac{\pi a}{s}\right) + \cos\left(\frac{\pi b}{s}\right)} \tag{135}$$

Also, for this case, $T_{bm} = T_3$. The geometry requirements, then, can be determined by combining Equations (123), (124), (125), and (135) to arrive at a relationship similar to Equation (126):

$$\left(\frac{\pi}{s}\right) \frac{\sin\left(\frac{\pi b}{s}\right)}{\cos\left(\frac{\pi a}{s}\right) + \cos\left(\frac{\pi b}{s}\right)} = \left(\frac{E}{305}\right)\left(\frac{L_c}{D_H^{1.2}\ G^{0.2}}\right)\left(\frac{T_3^{0.67}}{T_f^{0.56}}\right)\left(\frac{T_{s_{max}} - T_3}{T_3 - T_2}\right) \tag{136}$$

where T_f is defined as in Equation (130).

To determine which thermal design equations are applicable, a limiting relationship in terms of known variables must be developed. When x = L, the corresponding value of θ in terms of b can be found from Equation (115). Substituting this value of θ into Equation (119), a relationship between reactor temperatures and reactor power distribution for the case of $T_{s_{max}}$ being a mathematical maximum can be determined as follows:

$$\frac{T_{s_{max}} - T_3}{T_3 - T_2} \geq \frac{\sin^2\left(\frac{\pi b}{s}\right)}{\cos\left(\frac{\pi b}{s}\right)\left[\cos\left(\frac{\pi a}{s}\right) + \cos\left(\frac{\pi b}{s}\right)\right]} \tag{137}$$

One further check on the validity of the thermal design equations is necessary. The heat transfer coefficient relationship of Equation (123) is for turbulent flow. To insure that the flow through the coolant passage is turbulent, the Reynold's number (R_e) must be $\geq$10,000, or

$$R_e = \frac{D_H\ G}{\mu} \geq 10,000 \tag{138}$$

The case in which b = a leads to a symmetrical longitudinal power profile simplifying the relationships, allowing them to be plotted in a form for maximum engineering utility. A plot of four profiles, extending from the uniform profile to the isothermal fuel element profile and including a nominal profile adequate for initial design (2:1 sine) is given in Figures 2.3-2, 2.3-3, and 2.3-4. Figure 2.3-4 includes data which allows computation of the film temperature correction. A further refinement to improve engineering utility is given by the plots in Figures 2.3-5, 2.3-6, 2.3-7, and 2.3-8. The first three figures show the correlation for the 1:0 sine, 2:1 sine, and isothermal profiles, respectively; the last figure is a plot of correction factors needed to account for the dependence of air properties upon temperature level (increasingly larger correction is required as the air temperature at the reactor discharge departs from 1800°F). The choice of which presentation to use depends upon the particular problem under study. More accuracy can be obtained by using the more general, more complex relationships as plotted or given in nomogram form in reference 1.

1.2 Short-Form Pressure Ratio Calculation

The exact differential equation for the influence of friction and heat addition on compressible fluid flow is:

$$d(\ln P) = -\frac{\gamma M^2}{2}\left[\frac{4f}{D_H}\,dx + d(\ln T)\right] \qquad (139)$$

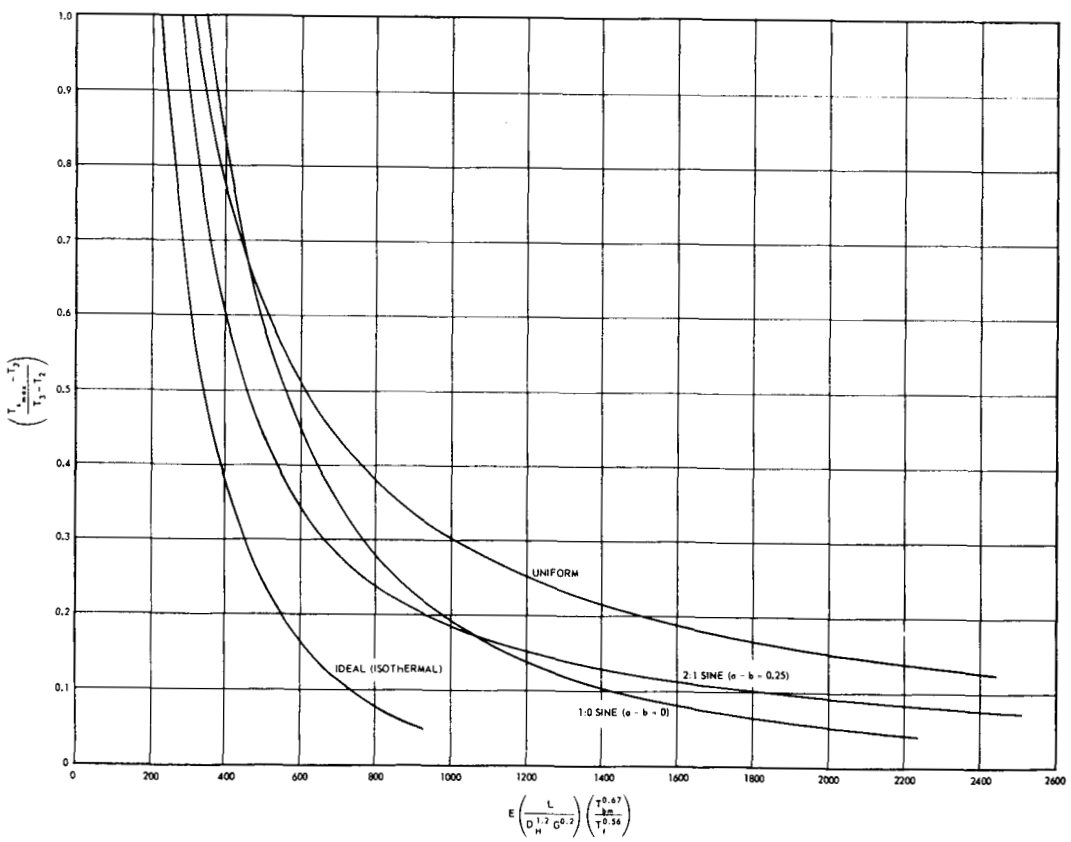

Fig. 2.3-2 – Plot of thermal sizing relationships for commonly used power distributions

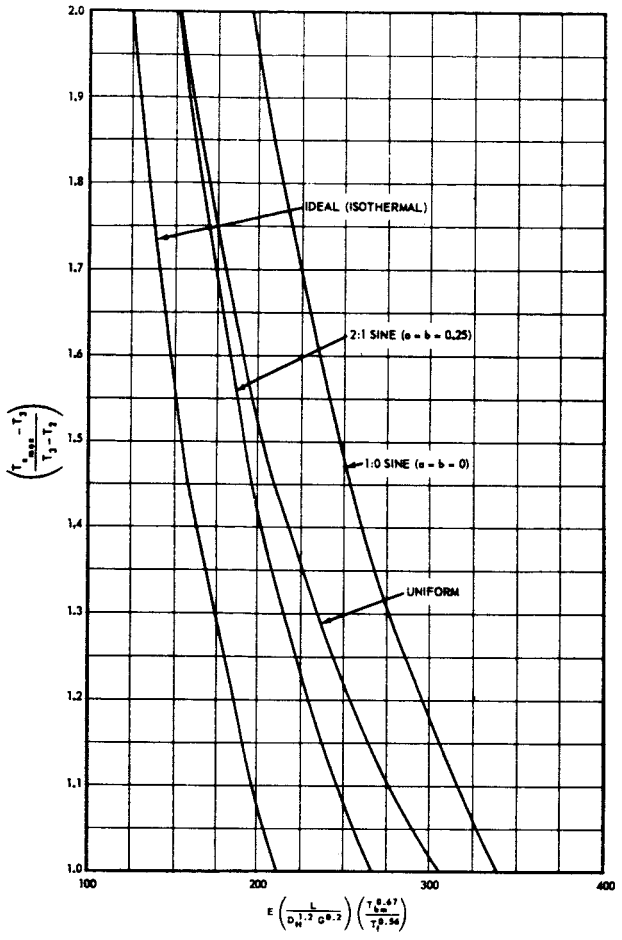

Fig. 2.3-3 – Plot of thermal sizing relationships for commonly used power distributions (extended range)

Equation (138) can be applied to the reactor core and integrated over the entire core to give:

$$\ln \frac{P_3}{P_2} = -\frac{\gamma M_{avg}^2}{2} \left[\frac{4fL_c}{D_H} + \ln\left(\frac{T_3}{T_2}\right)\right] \tag{140}$$

where M_{avg} = average value of Mach number in the coolant passage. Dimensional analysis of Equation (140) leads to:

$$\frac{P_3}{P_2} = B' \left(\frac{T_3}{T_2}, \sqrt{\frac{R}{\gamma C_p}}, \frac{G\sqrt{T_2}}{P_2}, \frac{f_{avg} L_c}{D_H}\right) \tag{141}$$

R is a constant for a particular gas. The temperature level T_2 accounts for the temperature dependence of γ and C_p. Therefore, the term $R/\gamma C_p$ can be eliminated from Equation (141). If f_{avg} can be written as a multiple of a "smooth tube" value:

$$f_{avg} = k\,(0.046\, R_e^{-0.2}) \tag{142}$$

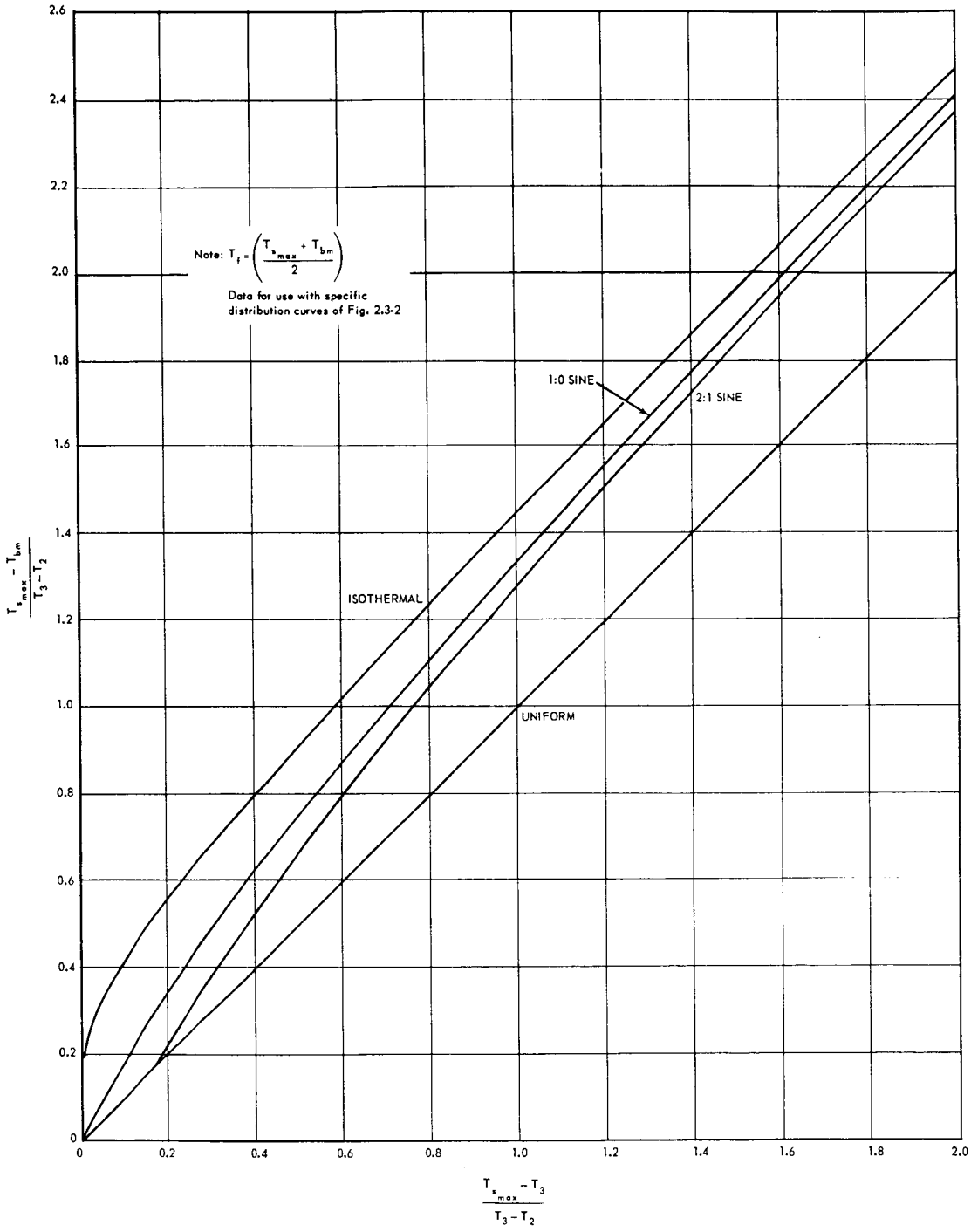

Fig. 2.3-4 – Plot for determination of requisite air temperature (T_{bm})

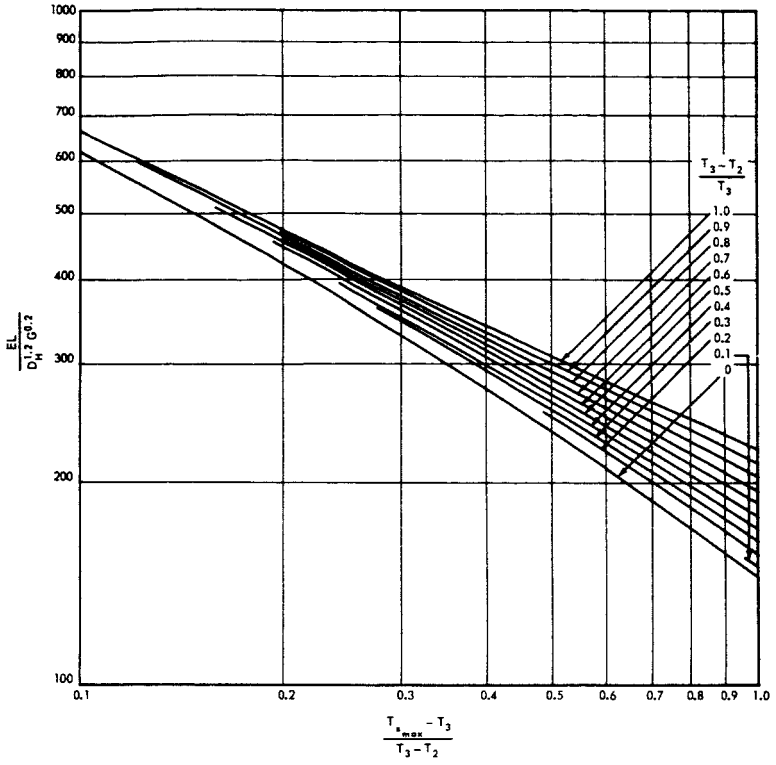

Fig. 2.3-5 – Plot of thermal sizing relationships for 1:0 sine curve

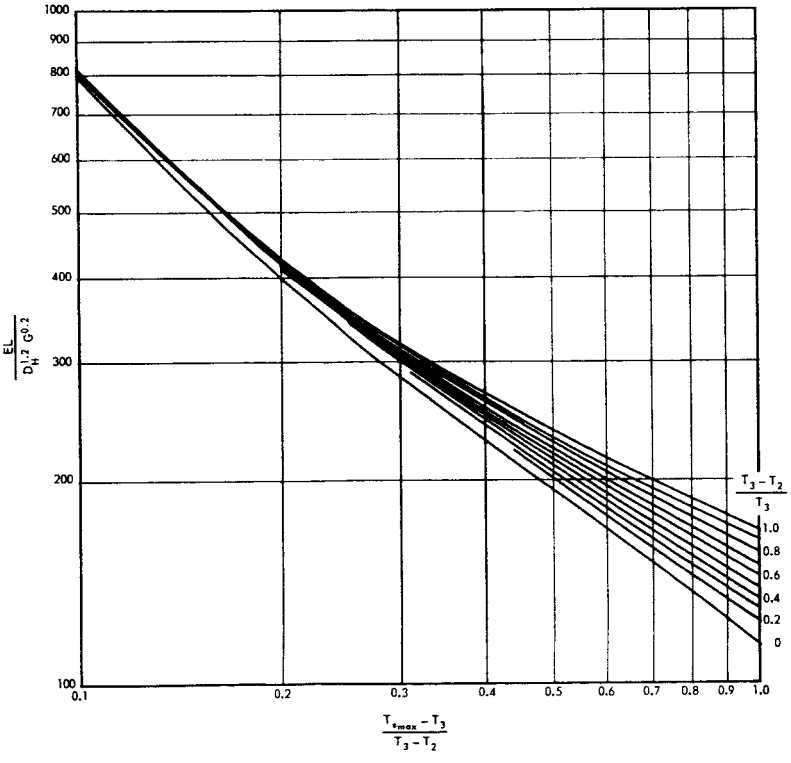

Fig. 2.3-6 – Plot of thermal sizing relationships for 2:1 sine curve

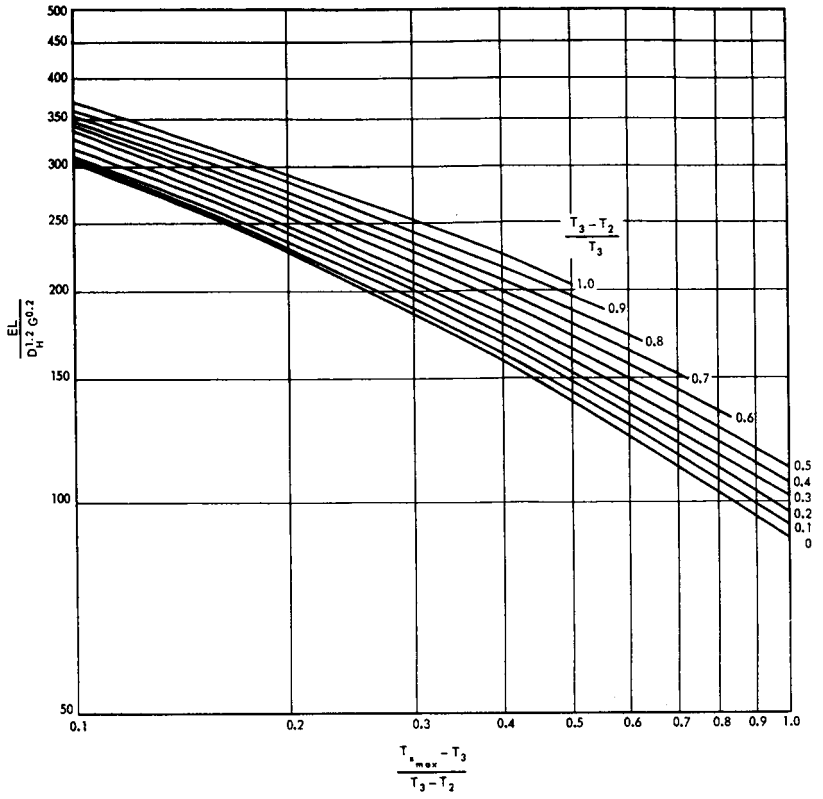

Fig. 2.3-7 – Plot of thermal sizing relationships for isothermal power distribution

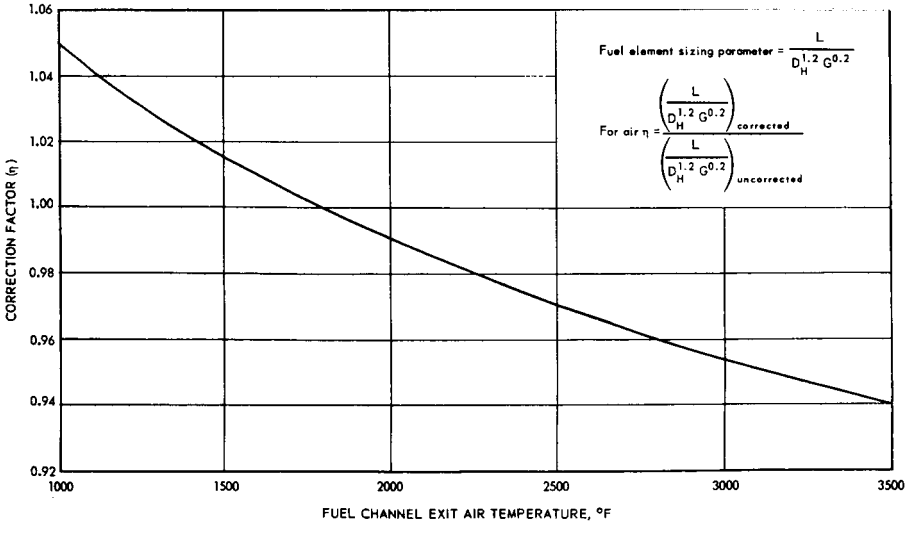

Fig. 2.3-8 – Correction factor for fuel element sizing parameter

When the equivalent for R_e from Equation (138) is substituted into Equation (142),

$$f_{avg} = \frac{0.046\ k\ \mu^{0.2}\ g^{0.2}}{D_H^{0.2}\ G^{0.2}} \tag{143}$$

When the variation of $\mu^{0.2}$ with temperature is neglected and Equation (143) is substituted into Equation (141):

$$\frac{P_3}{P_2} = B''\left(\frac{T_3}{T_2},\ \frac{G\sqrt{T_2}}{P_2},\ \frac{k\ L_c}{D_H^{1.2}\ G^{0.2}}\right) \tag{144}$$

The dimensionless groupings can be correlated to produce the following empirical relationships:

$$\left(\frac{G\sqrt{T_2}}{P_2}\right)^2\left(\frac{k\ L_c}{D_H^{1.2}\ G^{0.2}} + \psi\right) = \xi \tag{145}$$

where

$$\psi = \frac{101\left(\frac{T_3}{T_2} - \frac{P_3}{P_2}\right)}{\left(\frac{P_3}{P_2} - 0.100\right)\left(\frac{T_3}{T_2} + 0.111\right)}$$

$$\xi = 73.6\left[\frac{1 - \left(\frac{P_3}{P_2}\right)^2}{0.542 + \left(\frac{T_3}{T_2}\right)}\right]$$

The parameter $(L_c/D_H^{1.2}\ G^{0.2})$ was determined from the thermal design relationships for the reactor. Therefore, the mass velocity G can be calculated from Equation (145) for any combination of cycle variables, and the total reactor free flow area A_{ff} determined from the engine airflow as follows:

$$A_{ff} = \frac{W_2}{G} \tag{146}$$

Either of the coolant passage dimensions can be specified independently and the other calculated from the expression $L_c/D_H^{1.2}\ G^{0.2}$. However, there are physical limitations on allowable maximum and minimum values for coolant passage hydraulic diameter.

Computed solutions of the differential equation for the pressure relationship were run for air, with sufficiently small increments to achieve total pressure loss results within a maximum error of ±1 percent to determine the functions ξ and ψ. Approximately 1000 cases were run to establish validity of the functions for ranges of the individual variables as follows:

$0.1 \le D_H \le 0.4$ in.
$100 \le P_2 \le 400$ psia
$1000 \le T_2 \le 3000^{\circ}F$
$5 \le L \le 80$ in.
$0 \le G \le 1.2$ lb/sec-in.^{2}
$0 \le M_2 \le 0.3$
$0 \le M_3 \le 0.6$

but limited to $P_2/P_3 > 0.75$ and $T_3/T_2 < 2.3$.

The correlation was further limited by the assumption that the longitudinal power distribution in the reactor was symmetrical about the midplane, i.e., there was no forward or rearward bias of the relative power input to cause the average temperature of the coolant

to occur other than at the half-way point through the reactor. However, a correction factor can be applied to offset this effect.[2]

The final result is shown in Figures 2.3-9 and 2.3-10 for ξ and ψ, respectively.

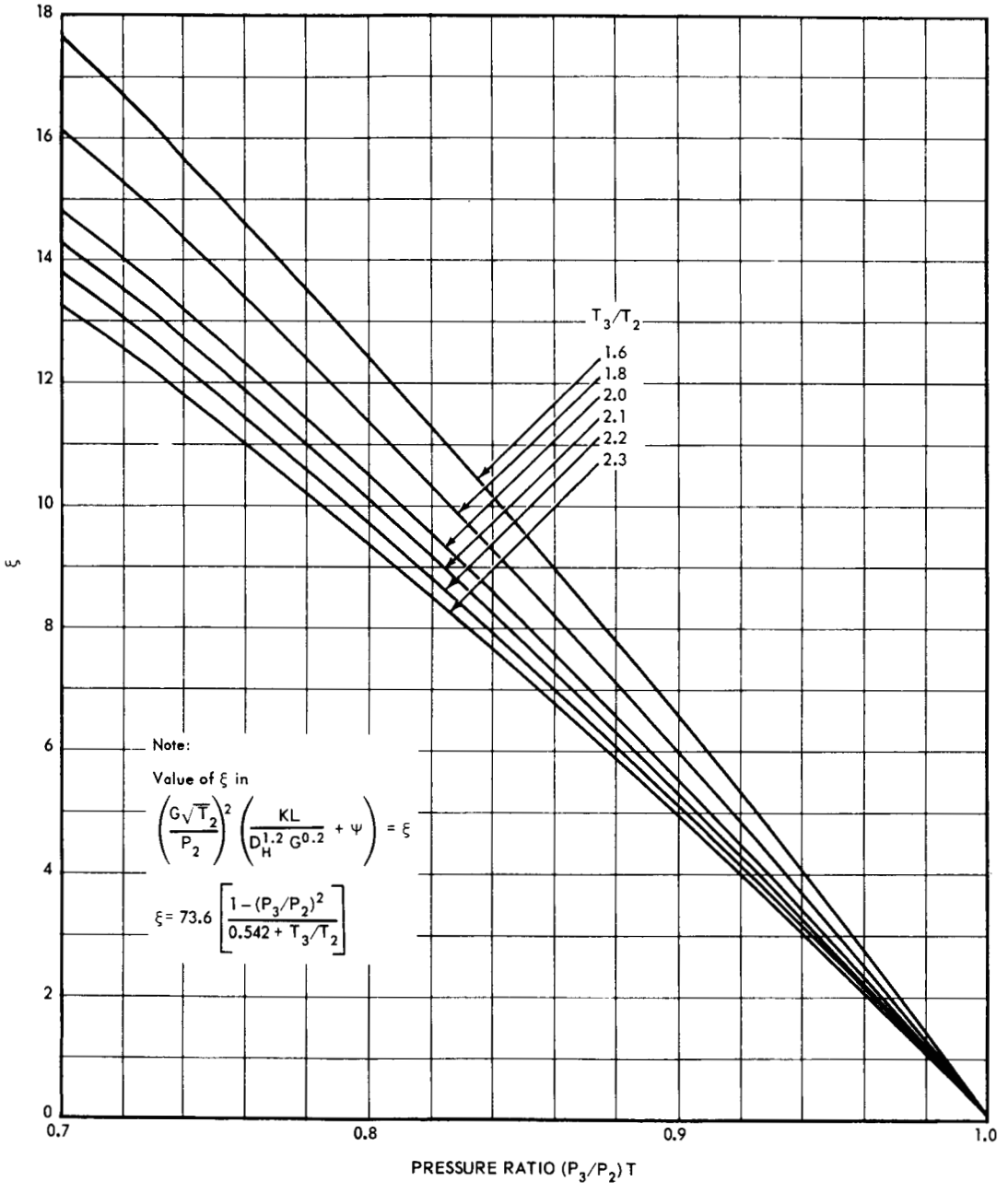

Fig. 2.3-9 – Pressure loss correlation for air, value of ξ

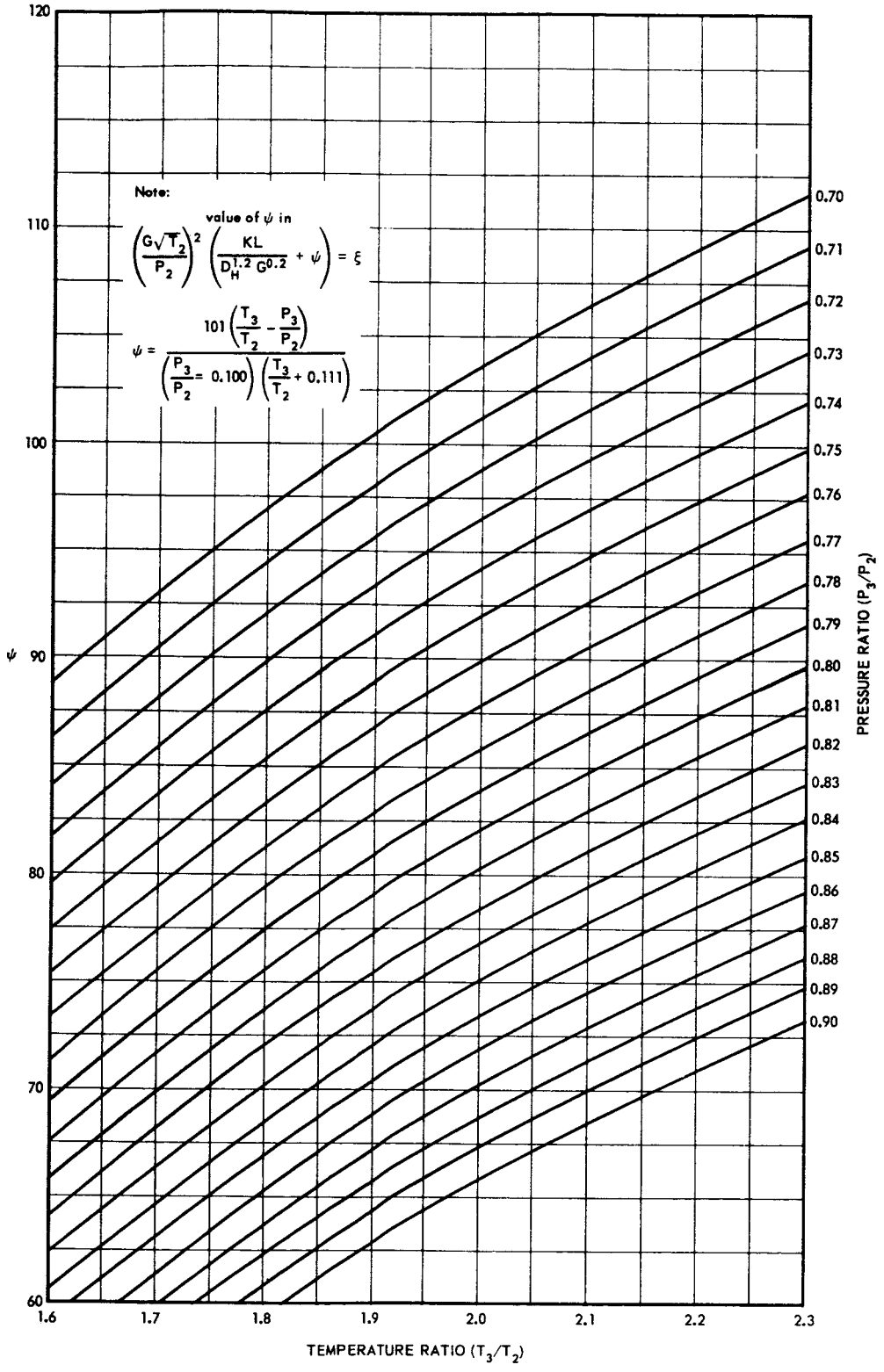

Fig. 2.3-10 – Pressure loss correlation for air, value of ψ

REFERENCES

1. Lapides, M., Motsinger, R., and Spera, R., "Generalized Thermal Design Relationships for Air in Conduits," GE-ANPD, DC 59-3-223, March 18, 1959.
2. Lapides, M., Motsinger, R., Mullikin, J., and Prickett, W., "Generalized Pressure Loss Computations for Heat Addition to Air Flowing in Constant Area Ducts," GE-ANPD, DC 60-5-57, May 11, 1960.

APPENDIX B-2

GENERALIZED THERMAL DESIGN AND PRESSURE LOSS RELATIONSHIPS FOR HEAT ADDITION TO HYDROGEN IN CONSTANT AREA DUCTS

By

R. J. Spera

Abstract

This Appendix presents graphical relationships between conduit geometry, power distribution, coolant flow rates, resultant temperatures and pressure loss for a gaseous hydrogen system. The data has its greatest utility in determining the channel geometry necessary to attain specified temperature and pressure conditions. A sample calculation has been included.

Introduction

Correlations have been developed which relate the temperature conditions and the pressure loss characteristics with the dimensions of constant area conduits for heat addition to an air medium. Graphical representations of these relations have been plotted for ease of application and are documented in references 1 and 2. The graphs have proven very useful in problems requiring the definition of channel dimensions to meet specified thermodynamic conditions. Indeed, this type of calculation can be performed with the graphs in a fraction of the time and cost required by computer methods and with the same accuracy. Consequently, the graphs have been profitably utilized to make preliminary sizing of reactor systems and to assess the relative effects of changes in various parameters on a particular characteristic of interest.

The need for a similar set of graphs for hydrogen arose with the advent of interest in nuclear reactors for rockets.

This appendix presents the data generated and describes its use with a sample calculation.

Summary

Figures B.1 to B.4 inclusive present data relating system temperature conditions and channel dimensions. Figures B.1, B.2, and B.3 are for particular longitudinal power distributions as follows:

(a) Figure B.1 - A normal sine curve distribution (commonly called a 1:0 distribution).
(b) Figure B.2 - A chopped sine curve distribution with a maximum-to-minimum power density ratio of 2 (commonly called a 2:1 distribution).
(c) Figure B.3 - An isothermal power distribution (one that results in a constant surface temperature).

These three power distributions are usually sufficient for the preliminary type of calculations performed with the generalized graphs. However, data for any other power distribution can be obtained with the air charts of reference 2 and the hydrogen to air correction curve of Figure B.4.

The geometry parameter, $EL/D_H^{1.2}\,G^{0.2}$, given as the ordinate value in Figures B.1, B.2, and B.3 must be corrected for hydrogen outlet temperature. The corrective curve is plotted in Figure B.5.

The pressure loss characteristics of hydrogen carrying channels was correlated by the same equation that described air systems, namely:

$$\left(\frac{G\sqrt{T_1}}{P_1}\right)^2 \left[\frac{KL}{D_H^{1.2}\,G^{0.2}} + \psi\right] = \xi$$

where ψ and ξ are functions of pressure ratio, P_o/P_i, and temperature ratio, T_o/T_i, only. Plots of ψ and ξ are given in Figures B.6 and B.7.

Nomenclature

A_{ff}	Free flow area of passage, $inch^2$
A_H	Passage surface area, $inch^2$
D_H	Passage hydraulic diameter, inches
C_P	Hydrogen heat capacity, Btu/lb-^oR

E — Ratio of passage to smooth tube heat transfer coefficient

f — Friction factor

G — Coolant mass velocity, W/A_{ff}, lbs/sec-inch^2

h — Heat transfer coefficient, Btu/sec-inch^2-^oR

K — Ratio of passage friction factor to smooth tube friction factor

L — Passage heated length, inches

P — Total pressures, psi

P_i = hydrogen inlet

P_o = hydrogen outlet

T — Temperatures, ^oR

T_i = hydrogen inlet

T_o = hydrogen outlet

T_{sm} = maximum-average surface

T_b = hydrogen bulk at locale of T_{sm}

T_f = hydrogen film at locale of T_{sm}

$$T_f = \frac{T_b + T_{sm}}{2}$$

W — Hydrogen flow rate, lbs/sec

η — Correction factor for hydrogen outlet temperature

ψ — A pressure drop parameter determined from computer solutions of the differential pressure loss equation

ξ — A pressure drop parameter determined from computer solutions of the differential pressure loss equation.

Assumptions and Restrictions

1. The duct friction factor, f, is expressed by the relation:

$$f = .046\ K\,(N_{RE})^{-0.2}$$

This implicitly limits the application of the curves to turbulent flow systems.

2. Duct entrance and exit losses are not included in the pressure drop.
3. Heat is added to the fluid along the total length of the channel with a sine distribution symmetric about the channel midpoint. Quantitative effects of assymetrical power distributions on the pressure drop were not obtained for hydrogen, but can be estimated from similar corrections for air on Figures 13 and 14 of reference 1.
4. The fully developed heat transfer coefficient for hydrogen was assumed to be described by the following equation taken from reference 3:

$$h = .002881 \frac{G^{0.8}}{D_H^{0.2}} \frac{T_b^{0.8}}{T_f^{.636}}, \quad \frac{Btu}{sec\text{-}ft^2\text{-}^oR}$$

5. The specific heat of hydrogen was assumed to be described by the following equation:

$$C_P = 1.6\ T^{.11}$$

Actually, this equation is not applicable below 1000^oR but most hydrogen systems have only a small fraction of their length in this temperature range so that resultant error is small.

Formulation Methods and Accuracy of Curves

The hydrogen thermal design curves of Figures B.1, B.2, and B.3 are theoretical modifications of similar air data in reference 1. The procedure used in obtaining them is outlined below.

In reference 2, it is shown that the parameter hA_H/WC_P is a function only of the temperature grouping $(T_{sm}-T_o/T_o - T_i)$ and the longitudinal power distribution of a heated channel. It follows then, that two systems, one hydrogen and one air, having the same temperature conditions and power distributions would have the same value of hA_H/WC_P. This parameter can be described by combining the definitions of each of its components; thus, for air,

$$\frac{hA_H}{WC_P} = .003278 \left(\frac{L}{D_H^{1.2} G^{0.2}}\right) \left(\frac{T_b^{.67}}{T_f^{.56}}\right)$$

as shown in reference 2. Making a similar evaluation for hydrogen using the equations for h and C_p listed in the previous section,

$$\frac{hA_H}{WC_P} = .004275 \left(\frac{L}{D_H^{1.2} G^{0.2}} \right) \frac{T_b^{.69}}{T_f^{.636}}$$

Equating the hydrogen and air parameters, it is obvious that the hydrogen geometry term, $(L/D_H^{1.2} G^{0.2})$ is related to the air geometry term by,

$$\left(\frac{L}{D_H^{1.2} G^{0.2}} \right)_{H_2} = .7665 \frac{T_f^{.076}}{T_b^{.02}} \left(\frac{L}{D_H^{1.2} G^{0.2}} \right)_{air}$$

For most temperature conditions of interest, $(T_f/T_b)^{.02}$ will have an approximate value of .995; therefore, the previous relation can be approximated by:

$$\left(\frac{L}{D_H^{1.2} G^{0.2}} \right)_{H_2} = .77 \, T_f^{.056} \left(\frac{L}{D_H^{1.2} G^{0.2}} \right)_{air}$$

This last equation is the basic relationship used to transform the air thermal curves of reference 1 to Figures B.1, B.2, and B.3 and the equation is plotted in graphical form on Figure B.4.

The percent error of Figures B.1, B.2, and B.3 when compared with computer program results may be as much as $\pm 5\%$. This is a cumulative error due in part to the inadequacy of describing the hydrogen properties by average values over the large temperature ranges of hydrogen systems and due in part to the inaccuracies in reading the air charts. The same type of information can be generated with much greater accuracy by correlating the data directly from a series of computer calculations.

The correlations of Figures B.1, B.2, and B.3 are necessarily based on a constant hydrogen outlet temperature. The correction curve of Figure B.5 was determined by a series of computer calculations using a constant 2:1 sine power distribution. The accuracy of the correction curve for other power distributions

was not evaluated.

The pressure drop parameters, ξ and ψ, of Figures B.6 and B.7 were determined from a large number of computer calculations after it was determined that the pressure drop in a hydrogen carrying channel could be correlated by equation of the form:[4]

$$\left(\frac{G\sqrt{T_i}}{P_i}\right)^2 \left[\frac{KL}{D_H^{1.2} G^{0.2}} + \psi\right] = \xi$$

Sample Calculation

A brief example will demonstrate the procedural use of the curves for sizing a system to specified thermal conditions.

Assume the problem is to determine the geometry of coolant channels required to meet the following conditions:

(a) Hydrogen inlet temperature, T_i, = $200^{\circ}R$

(b) Hydrogen outlet temperature, T_o, = $4000^{\circ}R$

(c) Hydrogen inlet pressure, P_i, = 650 psia

(d) Hydrogen outlet pressure, P_o, = 602 psia

(e) Hydrogen weight flow, W = 50.4 lbs/sec

(f) Maximum channel surface temperature, T_{sm} = $4765^{\circ}R$

(g) Assume channel friction factor ratio, K = 1.25

(h) Assume channel heat transfer ratio, E, = 1.0

(i) Longitudinal power distribution to be a 2:1 sine curve.

Step 1 - Compute temperature ratio parameter $(T_{sm}-T_o/T_o - T_i)$

$$\frac{(T_{sm}-T_o)}{(T_o - T_i)} = \frac{4765 - 4000}{4000 - 200} = \frac{765}{3800} = .2013$$

Step 2 - Compute temperature ratio parameter $(T_o - T_i)/T_o$

$$\frac{(T_o - T_i)}{T_o} = \frac{4000 - 200}{4000} = \frac{3800}{4000} = .95$$

Step 3 - Using Figure B.2, determine the value of $EL/D_H^{1.2} G^{0.2}$ as 485, and since E = 1, this is the value of $L/D_H^{1.2} G^{0.2}$.

Step 4 - Compute temperature ratio T_o/T_i

$$\frac{T_o}{T_i} = \frac{4000}{200} = 20$$

Step 5 - Compute pressure ratio, P_o/P_i

$$P_o/P_i = \frac{602}{650} = .926$$

Step 6 - Determine values of the pressure drop parameters ξ and ψ from Figures B.6 and B.7

$$\xi = .044$$

$$\psi = 158$$

Step 7 - Determine the value of the channel inlet flow function, $\frac{G\sqrt{T_i}}{P_i}$, from the pressure drop equation:

$$\left(\frac{G\sqrt{T_i}}{P_i}\right)^2 \left[\frac{KL}{D_H^{1.2} G^{0.2}} + \psi\right] = \xi$$

Substituting

$$\left(\frac{G\sqrt{T_i}}{P_i}\right)^2 = \frac{.044}{[1.25(485) + 158]} = \frac{.044}{761} = 5.78/10^{-5}$$

$$\frac{G\sqrt{T_i}}{P_i} = 7.57/-3$$

Step 8 - Determine the channel mass velocity G

$$G = \frac{G\sqrt{T_i}}{P_i} \times \frac{P_i}{\sqrt{T_i}}$$

$$G = 7.57/-3 \times \frac{650}{\sqrt{200}} = .348$$

Step 9 - Compute channel geometry ratio $L/D_H^{1.2}$

$$\frac{L}{D_H^{1.2}} = \left(\frac{L}{D_H^{1.2}\, G^{0.2}}\right) G^{0.2} = 485\,(.348)^{0.2} = 485\,(.8096) = 392.5$$

Step 10 - Compute system free flow area A_{ff}

$$A_{ff} = W/G = \frac{50.4}{.348} = 144.8 \text{ inch}^2$$

The problem results are:

Channel geometry ratio $L/D_H^{1.2} = 392.5$

Total channel free flow area $A_{ff} = 144.8 \text{ inches}^2$

This problem had originally been calculated with a computer program in the "other" direction; namely, a fixed geometry was analyzed for a given flow rate

and power distribution. The resultant temperatures and pressures were those used as input for the sample problem. The geometry used in the computer program was as follows:

Channel length, $L = 48$ inches

Channel diameter, $D_H = .175$ inch

Channel free flow area, $A_{ff} = 1\ ft^2\ (144\ inches^2)$

From this geometry, $L/D_H^{1.2} = 48/(.175)^{1.2} = 389$

The ratio of graphical to computer results for this particular set of conditions is:

$$L/D_H^{1.2} = 392.5/389 = 1.009$$

$$A_{ff} = 144.8/144 = 1.006$$

References

1. Lapides, M. et al, "Generalized Pressure Loss Computations for Heat Addition to Air Flowing in Constant Area Ducts," General Electric Company, Aircraft Nuclear Propulsion Department, DC 60-5-57, May 1960.

2. Lapides, M. et al, "Generalized Thermal Design Relationships for Air in Conduits," General Electric Company, Aircraft Nuclear Propulsion Department, DC 59-3-223, March, 1959.

3. Noyes, R.N. and Skirvin, S.C., "Thermodynamic Property Formulas for Gaseous Hydrogen," General Electric Company, Aircraft Nuclear Propulsion Department, DC 61-1-47, January, 1961.

4. Prickett, W.Z., "General Reactor Sizing Techniques, Vol. I, Aerothermodynamic Sizing", General Electric Company, Nuclear Materials and Propulsion Operation, APEX 723A.

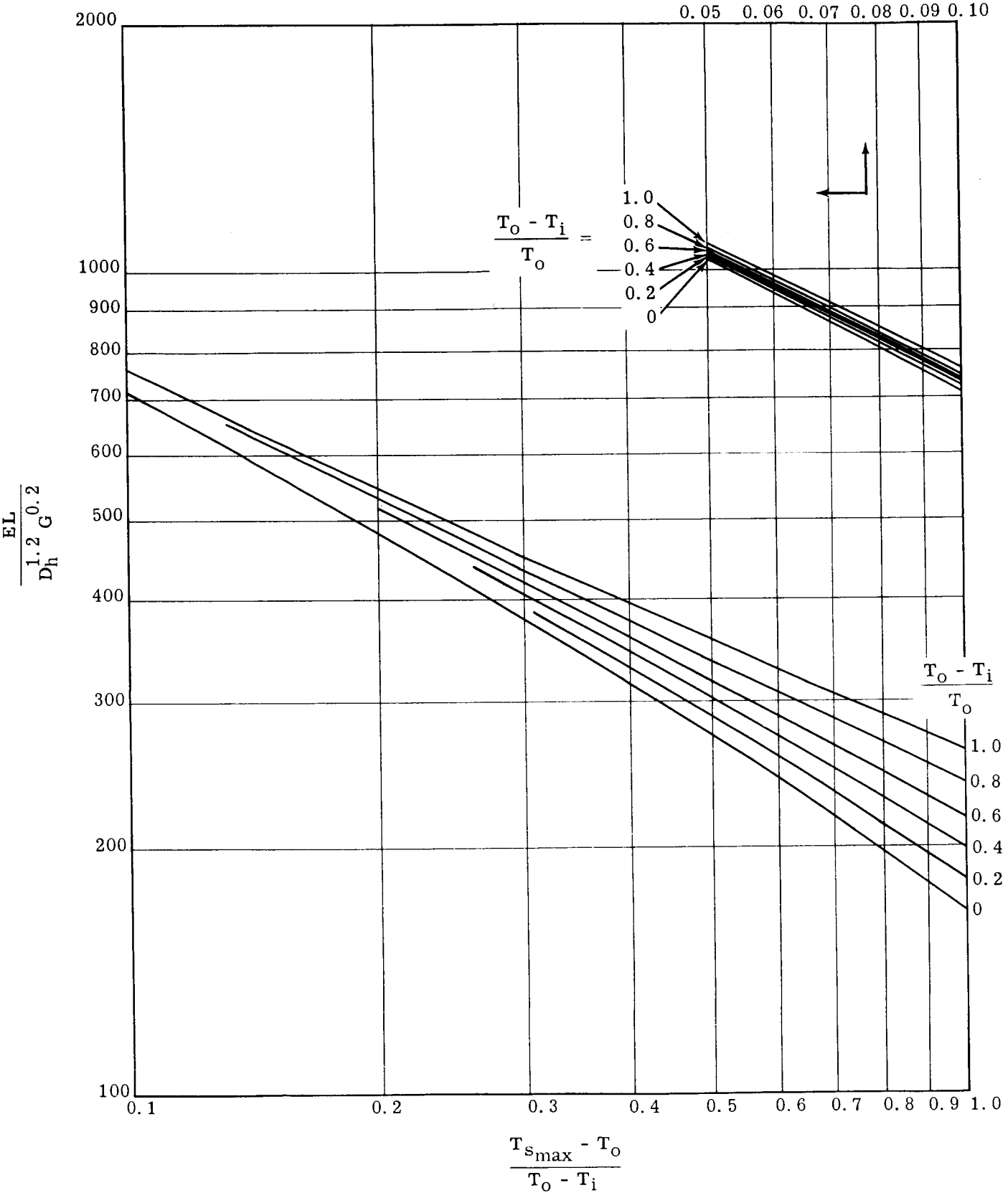

Fig. B-1 - Plot of hydrogen thermal sizing relationships for 1:0 sine curve

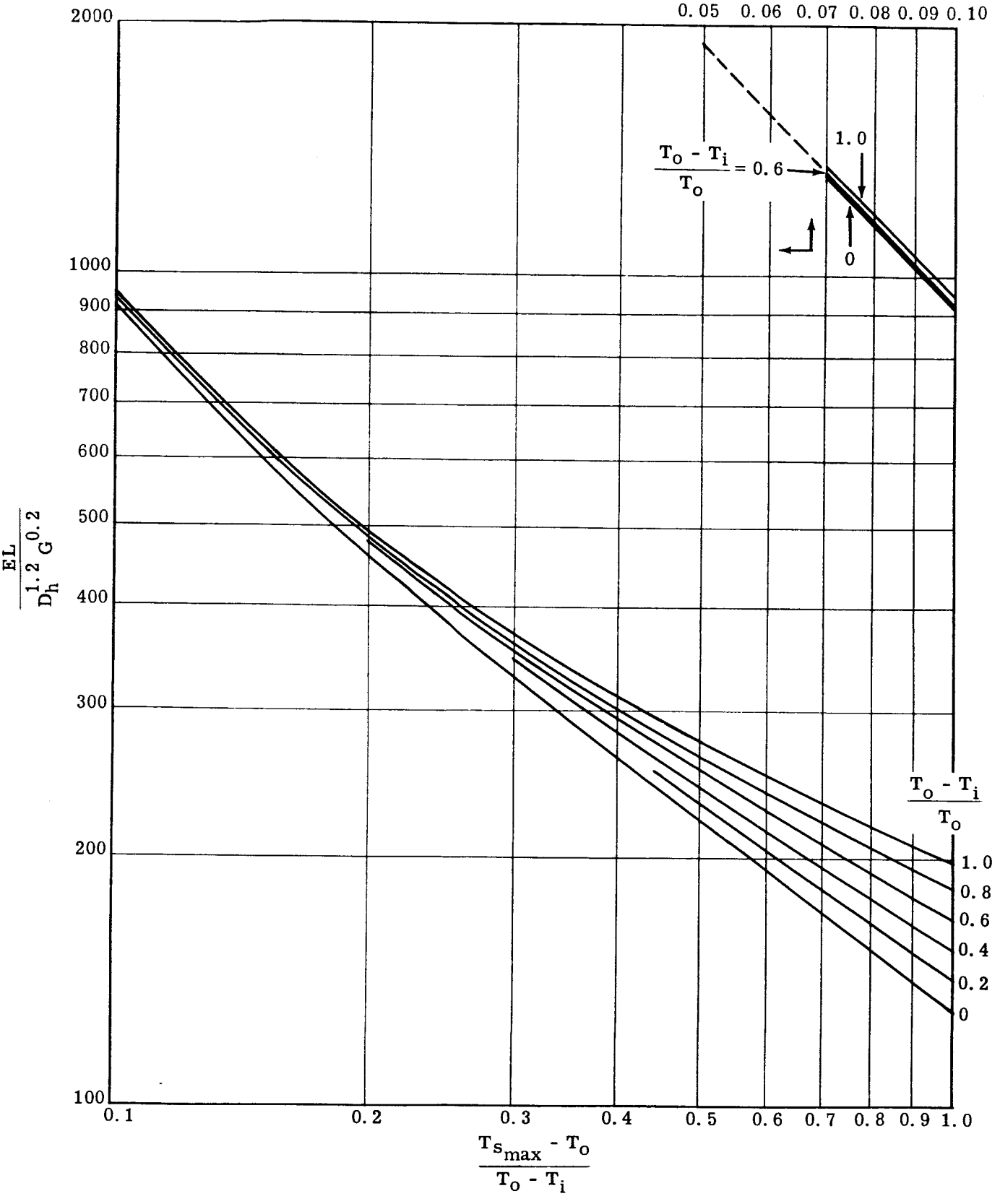

Fig. B-2 - Plot of hydrogen thermal sizing relationships for 2:1 sine curve

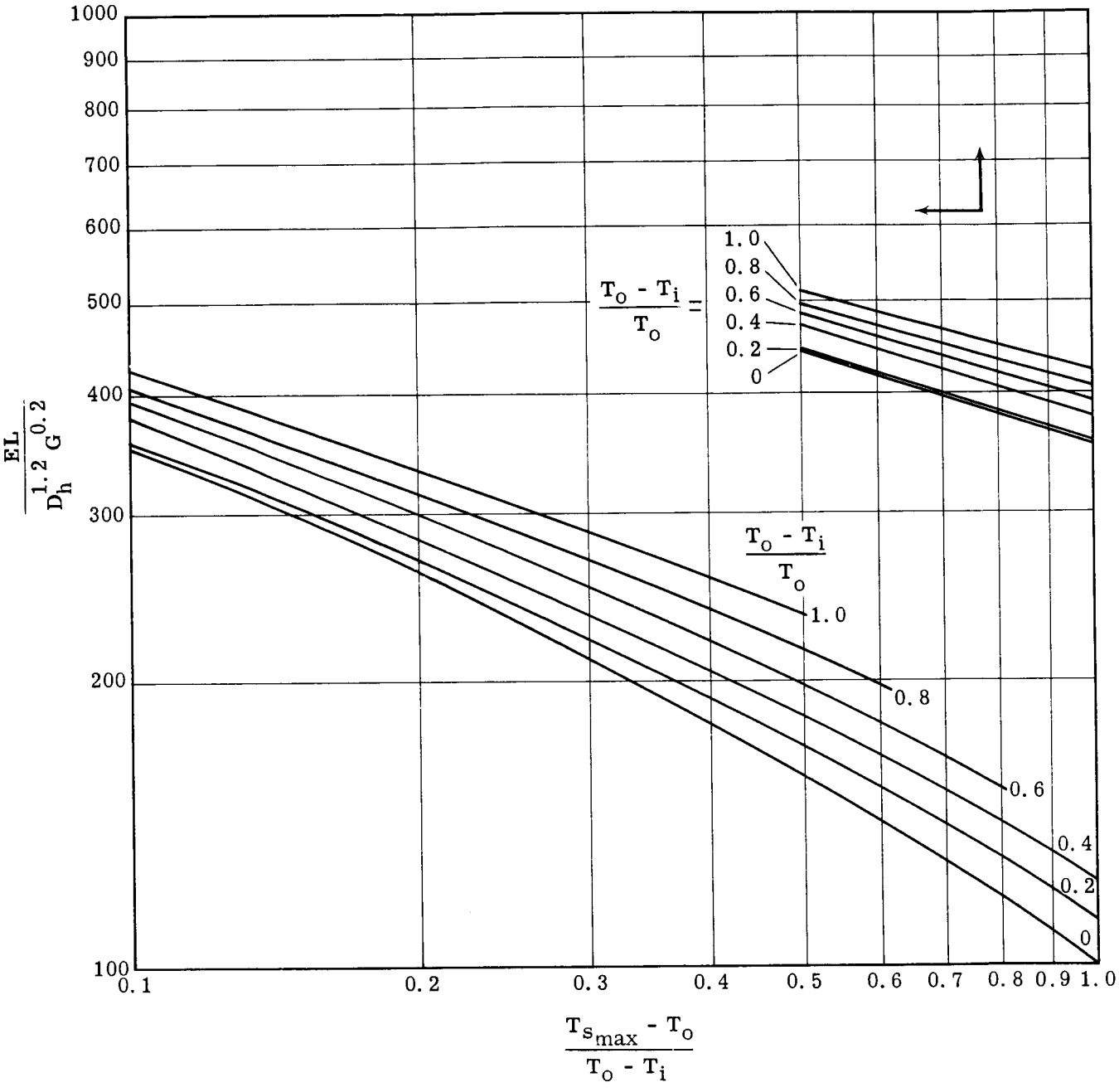

Fig. B-3 - Plot of hydrogen thermal sizing relationships for isothermal power distribution

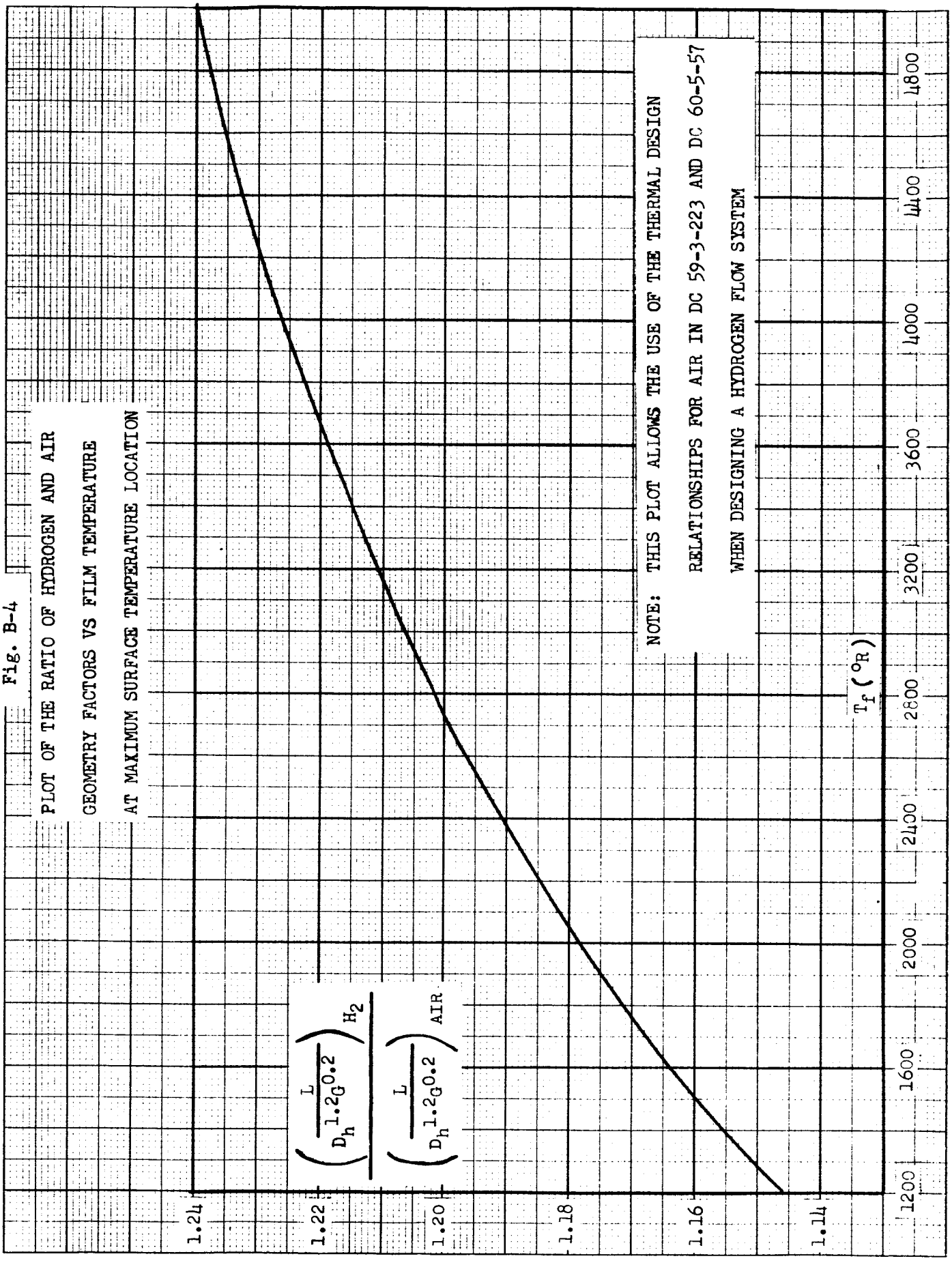
Fig. B-4
PLOT OF THE RATIO OF HYDROGEN AND AIR
GEOMETRY FACTORS VS FILM TEMPERATURE
AT MAXIMUM SURFACE TEMPERATURE LOCATION
$\left(\frac{L}{D_h^{1.2} G^{0.2}}\right)_{H_2} \Big/ \left(\frac{L}{D_h^{1.2} G^{0.2}}\right)_{AIR}$
1.24
1.22
1.20
1.18
1.16
1.14
1200
1600
2000
2400
2800
3200
3600
4000
4400
4800
T_f (°R)
NOTE: THIS PLOT ALLOWS THE USE OF THE THERMAL DESIGN
RELATIONSHIPS FOR AIR IN DC 59-3-223 AND DC 60-5-57
WHEN DESIGNING A HYDROGEN FLOW SYSTEM

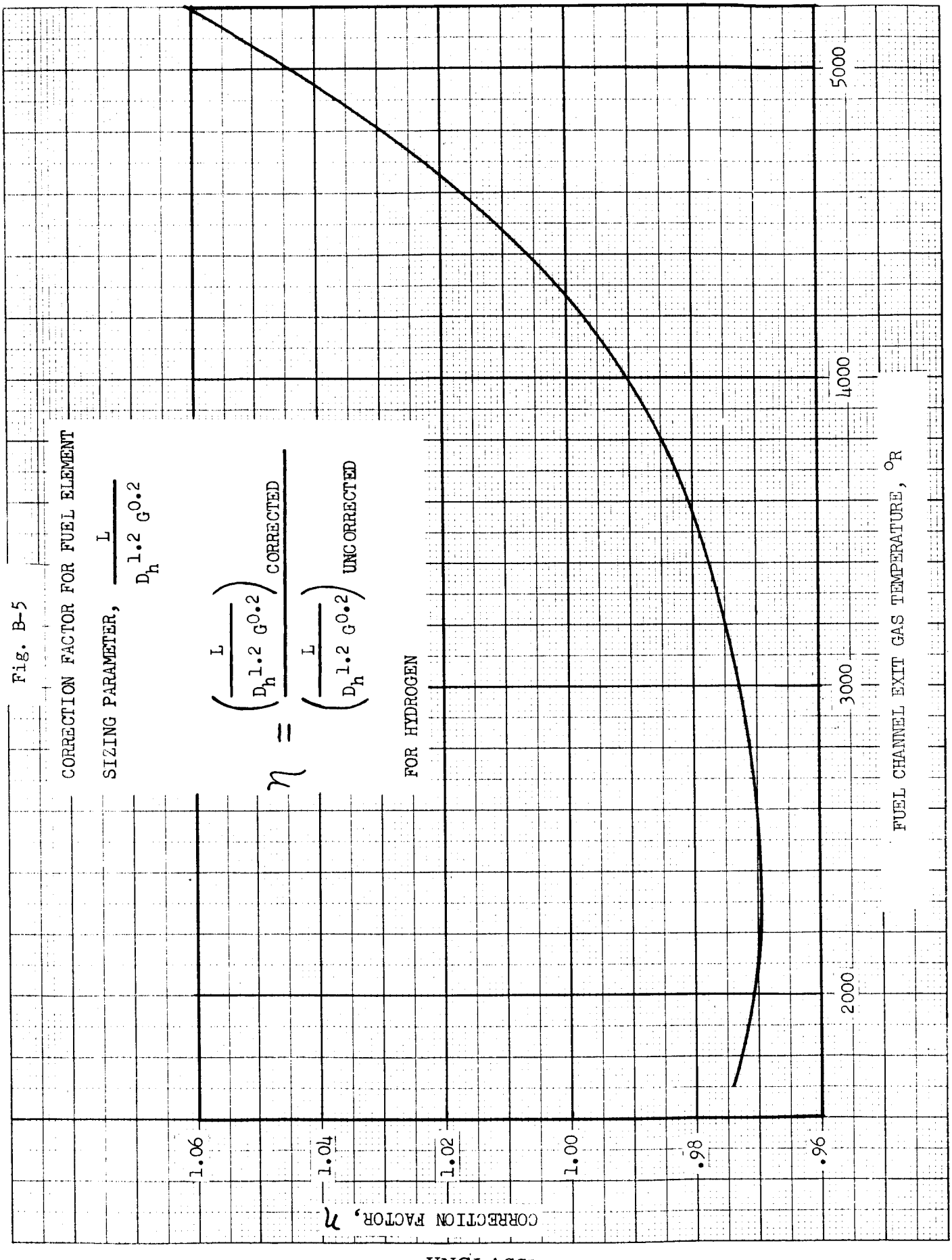
Fig. B-5
CORRECTION FACTOR FOR FUEL ELEMENT
SIZING PARAMETER, $\frac{L}{D_h^{1.2}\, G^{0.2}}$
$\eta = \left(\frac{L}{D_h^{1.2}\, G^{0.2}}\right)_{\text{CORRECTED}} \Big/ \left(\frac{L}{D_h^{1.2}\, G^{0.2}}\right)_{\text{UNCORRECTED}}$
FOR HYDROGEN
CORRECTION FACTOR, η
1.06
1.04
1.02
1.00
.98
.96
2000
3000
4000
5000
FUEL CHANNEL EXIT GAS TEMPERATURE, °R

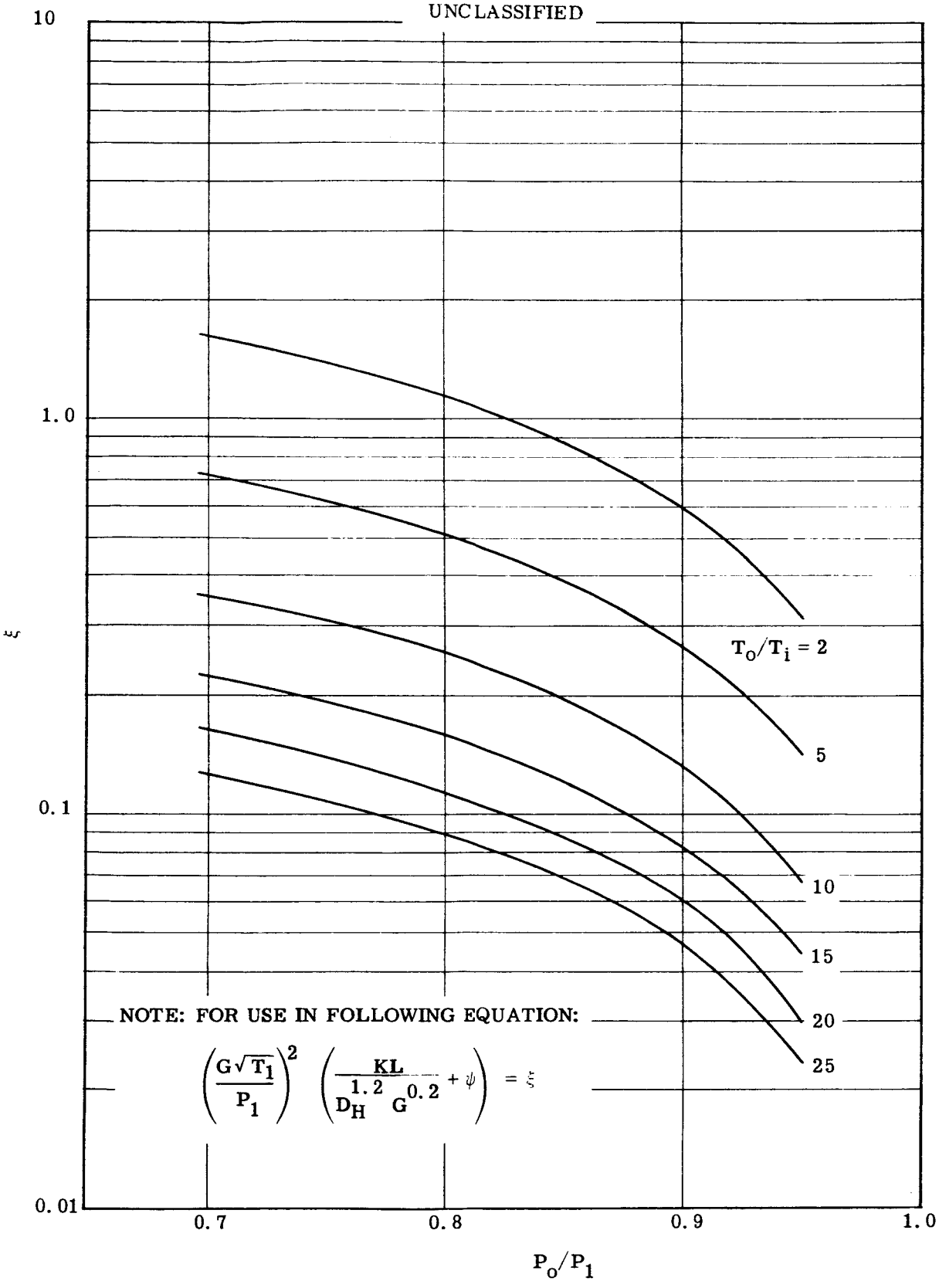

Fig. B-6 - Plot of ξ factor for hydrogen pressure drop generalization

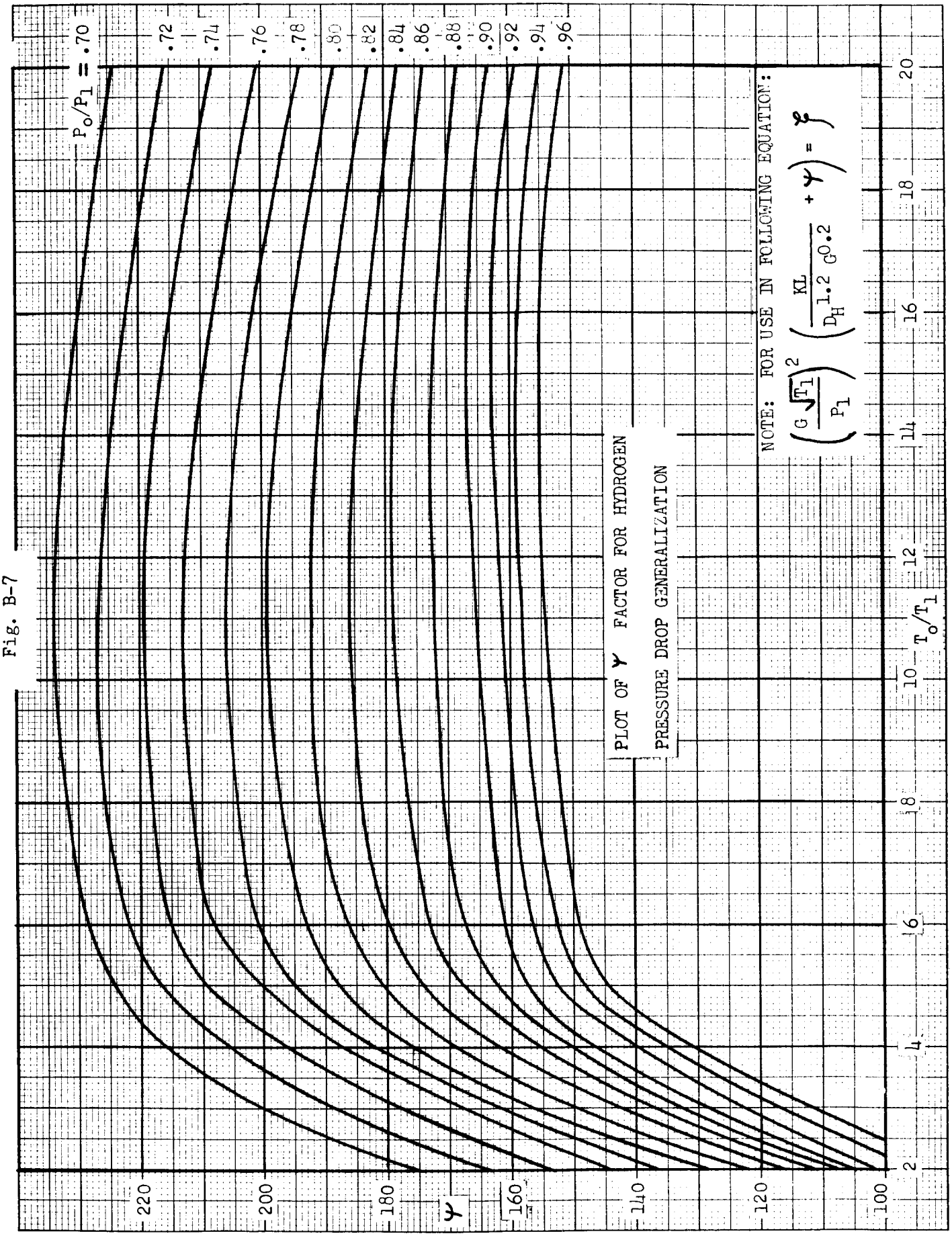
PLOT OF Y FACTOR FOR HYDROGEN
PRESSURE DROP GENERALIZATION
NOTE: FOR USE IN FOLLOWING EQUATION:
$\left(\frac{G\sqrt{T_1}}{P_1}\right)^2 \left(\frac{KL}{D_H^{1.2}\, G^{0.2}} + Y\right) = \mathcal{F}$
P_o/P_1 = .70 .72 .74 .76 .78 .80 .82 .84 .86 .88 .90 .92 .94 .96
Y
T_o/T_1
100 120 140 160 180 200 220
2 4 6 8 10 12 14 16 18 20

Fig. B-7

APPENDIX B-3*

1. NUCLEAR PROPERTIES

Simplified models for fixing the reactor size based upon the nuclear requirement can have great utility for initial assessment of feasibility. Since much nuclear information on critical mass is available for solid spherical geometries, a method for converting to the more practical cylindrical geometry with voids will be presented here, after presenting a sample of data for solid spheres.

The critical mass versus critical radius of a solid sphere[1] is shown for various ratios of moderator to fuel atoms U^{235} in Figures 2.3-11 through 2.3-15 for moderators consisting of H_2O, D_2O, C, Be, and BeO. These data are particularly useful base points for ideal systems in that the use of a moderator to save fuel is shown at the expense of size, hence, of weight. The data show consistent trends for each moderator, which may be summarized as follows:

1. The minimum size is achieved with no moderator.
2. As moderator is added in small amounts, an increase in size and an increase in critical mass results.
3. As more moderator is added, the critical mass decreases despite the larger volume because the effect of moderation becomes significant.

Note: This material is abstracted from APEX-800, Part A

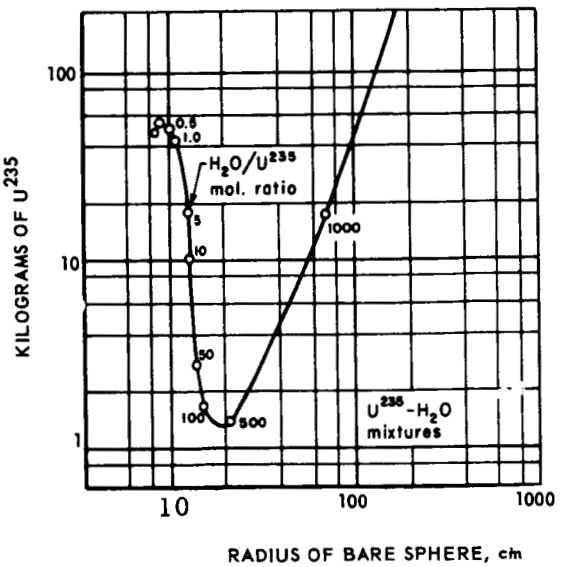

Fig. 2.3-11 – Characteristics of critical mixtures of U^{235} and H_2O

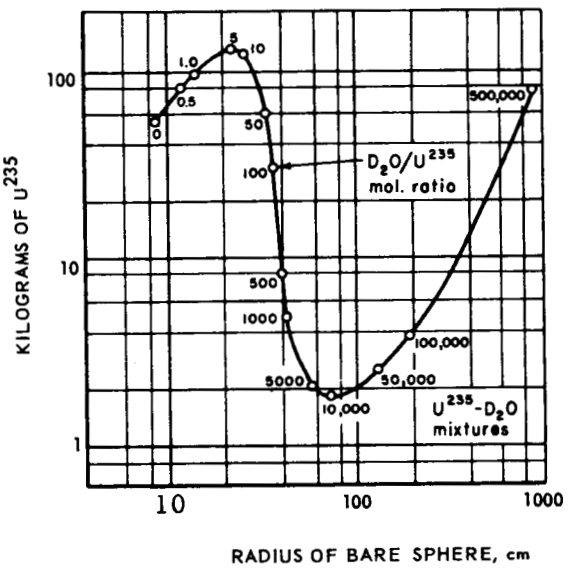

Fig. 2.3-12 – Characteristics of critical mixtures of U^{235} and D_2O

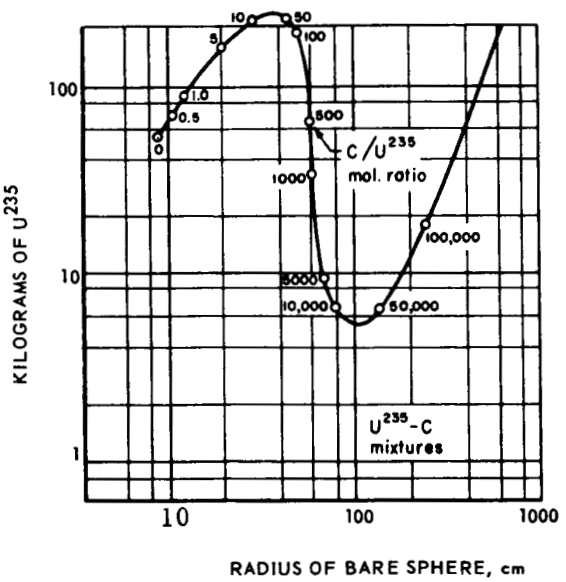

Fig. 2.3-13 – Characteristics of critical mixtures of U^{235} and C

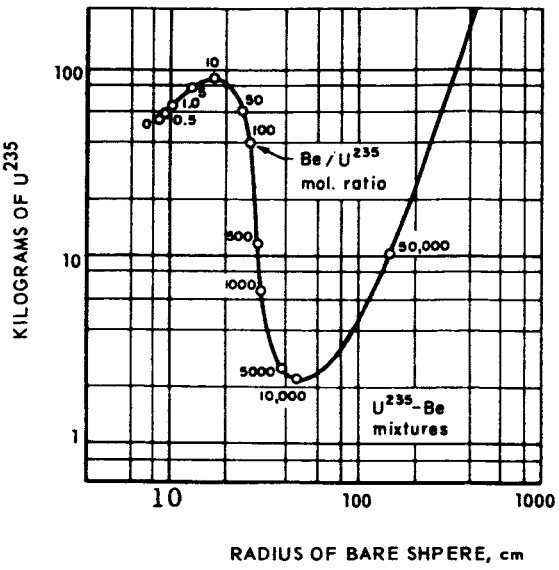

Fig. 2.3-14 – Characteristics of critical mixtures of U^{235} and Be

Fig. 2.3-15 – Characteristics of critical mixtures of U^{235} and BeO

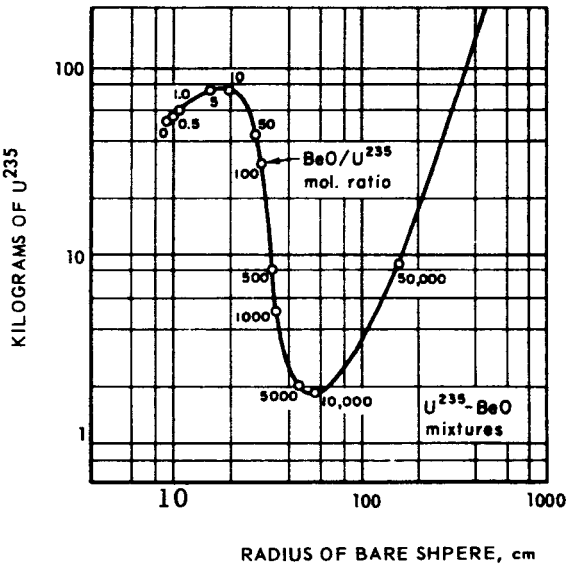

4. A minimum critical mass occurs when maximum benefit of moderator is achieved. At this point, the median energy of neutrons causing fissions has been reduced to the thermal energy level.
5. Further increase in moderator causes an increase in both critical mass and size because additional benefit from moderation is not possible.

These data are calculated results and should be supplemented wherever possible by experimental data. Furthermore, since the results presume homogeneous mixtures of fuel and moderator, cautions should be observed in making estimates of absolute magnitudes. However, trends are revealed which are helpful in establishing relative sizes.

Reference 2 presents the required information for direct sizing with U^{235} and BeO, including the effects of void and structural poison content.

The effects of introducing voids and of changing from spherical to cylindrical geometry are now discussed.

1.1 Effect of Homogeneous Void on the Critical Mass of a Reactor[3]

The introduction of a homogeneous void into a reactor of fixed composition increases both the size and the critical loading of the reactor. If the size and fuel inventory are known for a specific reactor having a given void fraction, the dimensions and fuel loading can be calculated for another reactor having the same relative materials composition but a different void fraction.

To determine the relationship between mass and radius in a reactor system without any void and a reactor having the same materials composition but with homogeneous void, the results given by the following derivation can be used. The reactor model chosen for this analysis was a bare, spherical reactor system, and the calculation scheme is the two-group, diffusion theory model. The steady state two-group diffusion theory equations are as follows:

$$-D_1 \nabla^2 \phi_1 + \Sigma_r \phi_1 = \eta \Sigma_a \phi_2 \tag{149}$$

$$-D_2 \nabla^2 \phi_2 + \Sigma_a \phi_2 = \Sigma_r \phi_1 \tag{150}$$

where

D = diffusion coefficient = $1/(3\Sigma_{tr})$
η = number of neutrons produced per neutron absorbed in the fuel
Σ_a = macroscopic thermal absorption cross section
Σ_r = macroscopic fast removal cross section
Σ_{tr} = macroscopic transport cross section
ϕ = neutron flux

The subscripts 1 and 2 refer to the fast and thermal groups, respectively.

The homogeneous parts of these two equations are wave equations of the form:

$$\nabla^2 \phi_1 + B^2 \phi_1 = 0 \tag{151}$$

$$\nabla^2 \phi_2 + B^2 \phi_2 = 0 \tag{152}$$

where B^2 is the geometric buckling of the system. For a spherical system:

$$B^2 = \left(\frac{\pi}{r+d}\right)^2 \tag{153}$$

where

r = radius of the core
d = extrapolation distance = $0.7104/\Sigma_{tr}$

Substituting Equations (151) and (152) into (149) and (150) reduces them to:

$$\left(\frac{1}{3\Sigma_{tr1}}\right) B^2 \phi_1 + \Sigma_r \phi_1 = \eta\Sigma_a \phi_2 \tag{154}$$

$$\left(\frac{1}{3\Sigma_{tr2}}\right) B^2 \phi_2 + \Sigma_a \phi_2 = \Sigma_r \phi_1 \tag{155}$$

The two-group equations for a reactor system containing void are identical to Equations (154) and (155) except that different materials constants are used.

The introduction of a homogeneous void into a reactor simply reduces the atomic concentration of all the materials by a factor of (1-V) where V is the void fraction. Consequently, the macroscopic cross sections will also be reduced by the same solid fraction:

$$\Sigma^* = \Sigma\ (1\text{-}V) = S\Sigma \tag{156}$$

where

Σ^* = macroscopic cross section for system with void
S = volume fraction of the solid material

The two-group equations for the dilute system are:

$$\left(\frac{1}{3\Sigma_{tr1}S}\right) B_V^2 \phi_1 + \Sigma_r S\phi_1 = \eta\Sigma_a S\phi_2 \tag{157}$$

$$\left(\frac{1}{3\Sigma_{tr2}S}\right) B_V^2 \phi_2 + \Sigma_a S\phi_2 = \Sigma_r S\phi_1 \tag{158}$$

where B_V^2 is the geometric buckling for the system with voids. Multiplying both Equations (157) and (158) by S yields:

$$\left(\frac{1}{3\Sigma_{tr1}}\right) B_V^2 \phi_1 + \Sigma_r S^2\phi_1 = \eta\Sigma_a S^2\phi_2 \tag{159}$$

$$\left(\frac{1}{3\Sigma_{tr2}}\right) B_V^2 \phi_2 + \Sigma_a S^2\phi_2 = \Sigma_r S^2\phi_1 \tag{160}$$

Equations (159) and (160) have the same relationships as Equations (154) and (155) and must reduce to that form for a critical system. Thus:

$$B_V^2 = S^2B^2 \tag{161}$$

From the expression for the geometrical buckling given in Equation (153) it can be shown:

$$r_V + d_V = \frac{1}{S}(r + d) \tag{162}$$

where the subscript V refers to the dimensions of the dilute system. Since $d_V = 0.7104/\Sigma_{tr}^* = d/S$, the expression for the radius of the dilute system is:

$$r_V = \frac{r}{S} = \frac{r}{(1\text{-}V)} \tag{163}$$

Once the relationship between the critical radii is known, it is relatively simple to determine the critical mass relationships. The mass of a spherical system is given by:

$$m = 4\pi r^3 \frac{\rho F_f M_f}{3M_m} \tag{164}$$

where

m = mass of the fissionable isotope
r = physical radius of the system
ρ = density of the fuel-bearing compound
F_f = volume fraction of the fuel-bearing compound
M_f = atomic weight of the fissionable isotope
M_m = molecular weight of the fuel-bearing compound

The only components in Equation (164) that change with the introduction of voids are F_f and r. The variation of r is expressed by Equation (163) and the variation in F_f is $F_{f_V} = (1-V)\ F_f$.

Consequently, the relationship between the critical mass of a system with voids, m_V, and the critical mass of a solid system, m, is:

$$m_V = \frac{m(1-V)}{(1-V)^3} = \frac{m}{(1-V)^2} \tag{165}$$

While this derivation is based on a one-region system, the same relationships hold, except for changes in geometry, for multiregion systems provided the increase in void fraction is the same in every region.

1.2 Effect of Geometry upon Bare Reactor Systems[3]

In this study, multigroup bare reactor calculations were performed for many single-region spherical reactors. To fully utilize the data, some relationship between the critical mass of a bare spherical system and that of an identical bare cylindrical system was developed. This relationship was obtained by considering the variation in geometric buckling of the two systems.

The difference in the critical mass of a bare cylindrical reactor and a bare spherical reactor with the same material composition is due only to the difference in system geometry and its effect on the leakage of the two systems. Leakage in two-group theory is expressed by $-D\nabla^2\phi$. Substituting $\nabla^2\phi = -B^2\phi$ from the wave equation, Equations (151) and (152) into the diffusion equation, Equations (149) and (150), gives $DB^2\phi$ for the leakage term where B^2 is the geometric buckling of the system. For spherical geometry, the geometric buckling B_S^2 is:

$$B_S^2 = \frac{\pi^2}{(r_S + d)^2} \tag{167}$$

where r_S is the radius of the sphere and d is the extrapolation distance. The sum $r_S + d$, is that point where the extrapolated neutron flux is assumed to be zero. The extrapolation distance is expressed as a function of the transport mean free path. This relationship, which is independent of reactor geometry, is taken as:

$$d = 0.7104\ \lambda_{tr} = \frac{0.7104}{\Sigma_{tr}} \tag{168}$$

where λ_{tr} is the transport mean free path and Σ_{tr} is the macroscopic transport cross section.

The geometric buckling for a bare cylindrical system, B_c^2, consists of an axial buckling term, B_{ca}^2 and a radial buckling term, B_{cr}^2. The two expressions for the axial and radial buckling are:

$$B_{ca}^2 = \frac{\pi^2}{(L+2d)^2} \tag{169}$$

$$B_{cr}^2 = \frac{\nu_o^2}{(r_c+d)^2} \tag{170}$$

where

L = length of cylinder
r_c = radius of a sphere
ν_o = first zero of the Bessel function $J_o = 2.405$

Thus, the total buckling for a bare cylindrical reactor is:

$$B_c^2 = B_{ca}^2 + B_{cr}^2 = \frac{\pi^2}{(L+2d)^2} + \frac{\nu_o^2}{(r_c+d)^2} \tag{171}$$

If two reactors have different geometries but the same materials composition, every constant in the diffusion equations for the two systems is identical except for the buckling term. Consequently, for both reactors to have the same eigenvalue, the two bucklings must be equal. Thus, the critical dimensions and loading of a bare cylindrical reactor can be determined if the critical size of a bare spherical reactor having the same materials composition is known.

1. Cylindrical reactor with an L/D = 1

The geometric buckling of a bare cylinder having an L/D of unity can be expressed as:

$$B_c^2 = \frac{\pi^2}{(2r_c+2d)^2} + \frac{\nu_o^2}{(r_c+d)^2} = \frac{\frac{\pi^2}{4}+\nu_o^2}{(r_c+d)^2} \tag{172}$$

Where $y = (r_c + d)$, then Equation (172) becomes:

$$B_c^2 = \frac{\nu_o^2 + \frac{\pi^2}{4}}{y^2} \tag{173}$$

The geometric buckling of a bare sphere having the same materials composition is:

$$B_s^2 = \frac{\pi^2}{(r_s+d)^2} \tag{174}$$

where extrapolation distance d is assumed to be identical for the two systems as expressed in Equation (162). When $x = (r_s + d)$, then Equation (174) becomes:

$$B_s^2 = \frac{\pi^2}{x^2} \tag{175}$$

Combining Equations (175) and (173), a relationship is established between the critical radius of a bare cylinder with L = D and that of a bare sphere.

$$B_s^2 = B_c^2 = \frac{\pi^2}{x^2} = \frac{\nu_o^2 + \frac{\pi^2}{4}}{y^2} \tag{176}$$

Dividing Equation (176) by π^2 and solving for y^2 gives:

$$y^2 = \left(\frac{\nu_o^2}{\pi^2} + \frac{1}{4}\right) x^2 = (0.586 + 0.25)\, x^2 = 0.836\, x^2 \qquad (177)$$

Taking the square root of both sides and substituting for x and y results in the determination of r_c in terms of r_s and d:

$$\begin{aligned} y &= 0.9143x \\ r_c + d &= 0.9143\,(r_s + d) \\ r_c &= 0.9143\, r_s - 0.0857\, d \end{aligned} \qquad (178)$$

The critical mass of a reactor is simply some density constant times the reactor volume. Consequently, the ratio of the critical mass of a bare cylinder, m_c, with L = D to that of a bare sphere m_s is:

$$\frac{m_c}{m_s} = \frac{2\pi r_c^3}{\left(4\pi r_s^3\right)} = 1.5\left(\frac{r_c}{r_s}\right)^3 \qquad (179)$$

Substituting Equation (178) in Equation (179) yields:

$$\frac{m_c}{m_s} = 1.5\left[0.9143 - 0.0857\left(\frac{d}{r_s}\right)\right]^3 \cong 1.1464 - 0.3224\left(\frac{d}{r_s}\right) \qquad (180)$$

2. Cylindrical Reactor with an L/D ≅ 1.5

It is difficult to develop the mass interrelationships for a cylinder with an L/D of 1.5 because of the extrapolation distance, d. If the length is slightly increased so that L = (1.5 D) + 1, the mass and radius relationships are easily obtained.

The critical dimension and the mass relationships between a bare spherical reactor and a bare cylindrical reactor of identical composition and an L = 1.5 D + d are obtained from the same relationships as that for the cylinder with L = D. The only change is made in the axial buckling term which becomes $(\pi/3y)^2$ instead of $(\pi/2y)^2$. Solving these equations gives the following functions:

$$r_c = 0.835\, r_s - 0.165\, d \qquad (181)$$

and

$$\frac{m_c}{m_s} \cong 1.310 - 0.7765\,\frac{d}{r_s} \qquad (182)$$

3. Cylindrical Reactor with L/D ≅ 2

As in the case where L/D = 1.5, the mass and radius interrelationships for an L/D of 2 become quite involved. However, if a slightly longer reactor is considered, where L = 2(D+d), the interrelationships between a bare cylindrical reactor and a bare spherical reactor are easily obtained. These functions are:

$$r_c = 0.8053\, r_s - 0.1947\, d$$

and

$$\frac{m_c}{m_s} \cong 1.5673 - 1.3747\,\frac{d}{r_s}$$

While this work given here is only for bare reactors, the analysis can be extended to include reflected reactors, by utilizing the principle of reflector savings. In effect, use of this principle transforms a two-region system into a one-region system. In this extension, care must be exercised in the manipulation of the savings term.

REFERENCES

1. Safenov, G., "Survey of Reacting Mixtures Employing U^{235}, Pu^{239}, and U^{233} for Fuel and H_2O, D_2O, C, Be, and BeO for Moderator," RAND Corporation, R-259, January 8, 1954.
2. Prickett, W. Z., "General Reactor Sizing Techniques, Vol. II, General Nuclear Sizing Techniques for Beryllia-Moderated Reactor," GE-ANPD, APEX-723B, July 1961.
3. Culp, A. W., et al., "Parametric Analysis of Some Fast Oxide-Fueled Systems with Moderating Reflectors," ASTRA, Inc., GE-ANPD, APEX-602, June 1, 1959.